Free Radical Biology and Medicine xxx (xxxx) xxx–xxx

Contents lists available at ScienceDirect

Free Radical Biology and Medicine

journal homepage: www.elsevier.com/locate/freeradbiomed

Original article

# *In vivo* assessment of reactive oxygen species production and oxidative stress effects induced by chronic exposure to gamma radiation in *Caenorhabditis elegans*

Erica Maremonti[a,c,*], Dag Markus Eide[b,c], Lisa M. Rossbach[a,c], Ole Christian Lind[a,c], Brit Salbu[a,c], Dag Anders Brede[a,c]

[a] Faculty of Environmental Sciences and Natural Resource Management (MINA) Norwegian University of Life Sciences (NMBU), 1432 Ås, Norway
[b] Norwegian Institute of Public Health, Lovisenberggata 8, 0456, Oslo, Norway
[c] Centre for Environmental Radioactivity (CoE CERAD), 1432 Ås, Norway

ARTICLE INFO

*Keywords:*
Ionizing gamma radiation
*Caenorhabditis elegans*
*In vivo* redox sensors
Reactive oxygen species
Mitochondrial dysfunction

ABSTRACT

In the current study, effects of chronic exposure to ionizing gamma radiation were assessed in the radioresistant nematode *Caenorhabditis elegans* in order to understand whether antioxidant defences (AODs) could ameliorate radical formation, or if increased ROS levels would cause oxidative damage. This analysis was accompanied by phenotypical as well as molecular investigations, via assessment of reproductive capacity, somatic growth and RNA-seq analysis.

The use of a fluorescent reporter strain (*sod1::gfp*) and two ratiometric biosensors (*HyPer* and *Grx1-roGFP2*) demonstrated increased ROS production ($H_2O_2$) and activation of AODs (SOD1 and Grx) *in vivo*. The data showed that at dose-rates $\leq$10 mGy $h^{-1}$ defence mechanisms were able to prevent the manifestation of oxidative stress. In contrast, at dose-rates $\geq$40 mGy $h^{-1}$ the continuous formation of radicals caused a redox shift, which lead to oxidative stress transcriptomic responses, including changes in mitochondrial functions, protein degradation, lipid metabolism and collagen synthesis. Moreover, genotoxic effects were among the most over-represented functions affected by chronic gamma irradiation, as indicated by differential regulation of genes involved in DNA damage, DNA repair, cell-cycle checkpoints, chromosome segregation and chromatin remodelling. Ultimately, the exposure to gamma radiation caused reprotoxic effects, with > 20% reduction in the number of offspring per adult hermaphrodite at dose-rates $\geq$40 mGy $h^{-1}$, accompanied by the down-regulation of more than 300 genes related to reproductive system, apoptosis, meiotic functions and gamete development and fertilization.

## 1. Introduction

Exposure to ionizing radiation can cause harmful toxic effects either by direct energy deposition onto biomolecules or by indirect damage through the production of free radicals [62]. The indirect effects proceed through a chain of physical and chemical events which leads to the production of free-radicals due to dissociation of water molecules, and thus to a dose-dependent formation of reactive oxygen species (ROS), such as superoxide ($O_2^{\cdot-}$), hydroxyl radicals (HO·), hydrogen radicals (H·) and hydrogen peroxide ($H_2O_2$) [63,68,82]. These radicals are continuously produced in the cells of organisms during exposure to ionizing radiation, and increased ROS levels have been measured in a wide range of species, including the green algae *Chlamydomonas reinhardtii*, the aquatic macrophyte *Lemna minor* and zebrafish [30,40,81]. Despite a short (nanoseconds) half-life [7], the formation of ionizing radiation-induced radicals has shown to increase persistently in the cells during prolonged exposures [15,74]. This may result in changes of the cellular redox balance, which can lead to the perturbation of essential biochemical processes including metabolism [26]. For instance, radiation may cause mitochondrial dysfunction, by compromising the electron transport chain (ETC), which exacerbates endogenous ROS production and the formation of oxidative stress condition [62]. Increased generation of mitochondrial ROS following low-dose irradiation plays multiple roles in signalling cascades and mediates apoptosis, thus may contribute significantly to cell survival [4]. Accordingly, oxidative damage to essential biomolecules, including DNA,

* Corresponding author. Faculty of Environmental Sciences and Natural Resource Management (MINA) Norwegian University of Life Sciences (NMBU), 1432 Ås, Norway.
*E-mail address:* erica.maremonti@nmbu.no (E. Maremonti).

https://doi.org/10.1016/j.freeradbiomed.2019.11.037
Received 30 September 2019; Received in revised form 21 November 2019; Accepted 28 November 2019

lipids and proteins are important contributors to the late effects following exposure to ionizing radiation [4,24,29,35,69]. Therefore, it is becoming increasingly evident that not only the indirect effects during the exposure itself, but even the subsequent production of free radicals plays a significant role to the overall biological effects of this stressor. Hence, detailed investigations into the role of ROS and the changes in the redox status produced following the exposure to ionizing radiation is of high importance.

At the species level, radiosensitivity ranges over several orders of magnitude [77]. It has been postulated that the ability of an organism to tolerate ionizing radiation is dependent on the efficiency of DNA repair mechanisms, and robust antioxidant defences to mitigate ROS and prevent oxidative stress [19].

The nematode *Caenorhabditis elegans* is amongst the most radioresistant organisms and is frequently used in radiation biology studies, particularly the post-mitotic stage can tolerate high doses of both X-ray and gamma radiation [13,31,34,46]. Interestingly, *C. elegans* possesses a wider range of antioxidant defences (AODs), compared to most organisms [22,27]. Among these, the glutathione peroxidases (GPx) play an important role in oxidative stress defence, through ROS scavenging. Glutathione (GSH) is therefore central to the maintenance of cellular redox homeostasis [5,80]. Measurement of the ratio between the oxidized to reduced [GSSG]/[2GSH] form of GSH has been shown to be a reliable proxy for oxidative stress manifestation [10,11,70]. Due to its highly specialized ROS and redox control system [11], *C. elegans* presents a suitable model for studying radiation induced ROS production, besides being a well-defined model organism for genetics and cell biology [38].

Therefore, in the current study, we investigate the effects of chronic exposure to gamma radiation on the accumulation of free radicals and the subsequent antioxidant responses in relation to apical reproductive and developmental effects in the nematode *C. elegans*. Furthermore, we examined the changes on the transcriptome upon irradiation during the entire larval development, in order to identify cellular and molecular functions related to the observed adverse effects and mechanisms mediating tolerance to ionizing radiation.

## 2. Material and methods

### 2.1. Culture and maintenance of nematodes

Synchronised cohorts of nematodes were maintained in continuously shaking liquid cultures at 20 °C in the dark [49]. The following strains were used: N2, wild type (Bristol) (*Caenorhabditis Genetic Centre*, Minneapolis, USA); *sod1::gfp* transgene, (GA508 wuIs54[pPD95.77 sod-1:GFP, rol-6(su1006)] (Institute of Healthy Ageing Genetics, University College London) [22]; $H_2O_2$ biosensor (HyPer) *(jrIs1[Prpl-17::HyPer];* [GSSG]/[2GSH] biosensor (*jrIs2[Prpl-17::Grx1-roGFP2])* [5].

Synchronization of nematodes was performed prior exposure to gamma radiation by alkaline hypochlorite treatment [61]. To facilitate hatching, eggs were suspended in 1 ml M9 buffer and placed on NGM-Petri dishes overnight.

Viability and hatching of L1 stage nematodes was assessed prior the start of the exposure.

### 2.2. Exposure to gamma radiation

The external gamma radiation exposure was conducted at the FIGARO $^{60}$Co irradiation facility (maximum permissible activity 400 GBq) at the Norwegian University of Life Sciences (NMBU) [50]. Nematodes were exposed, in triplicate, in liquid media (15 ml tissue-culture flasks or front row 24-well cell culture plates) or on NGM-Petri dishes (Ø 6 cm) [61] containing 15 or 0.5 ml of fresh *Escherichia coli OP50* (cultured overnight at 37 °C in L-Broth medium, [49]), respectively, re-suspended in moderately hard reconstituted water (MHRW) plus cholesterol [76] at pH 7.5 [45].

During exposure, controls were placed, in triplicate, behind lead shielding, while exposure containers were placed at distances corresponding to a calculated average absorbed dose-rates to water of 0.43–1.1 – 10.8–40.8 and 99.9 mGy $h^{-1}$ (Table S8 for dose-rates and respective total doses). Field dosimetry (air kerma rates measured with an ionization chamber) was traceable to the Norwegian Secondary Standard Dosimetry Laboratory (Norwegian Radiation Protection Authority, DSA, Oslo, Norway) [8]. Air kerma rates were measured using an Optically Stimulated Luminescence (OSL) based nanoDots dosimetry system (Landauer®) by positioning the dosimeters at the front and back of the experimental units. Dose-rates to water, calculated according to Lindbo Hansen E. [51]; were used as a proxy for dose-rates to the nematodes.

### 2.3. Effects on somatic growth and reproduction

N2 nematodes were used to assess phenotypic endpoints (growth, fertility and reproduction) by performing standard 96 h toxicity tests in 24-well cell culture plates, carried out at 20 °C in the dark [41]. Organisms (n = 12 ± 5 per well) were exposed to gamma radiation from L1 stage in triplicates.

For sampling, nematodes were stained with 0.5 ml of Rose Bengal (0.3 g/L) and placed for 10 min at 80 °C. Plates were stored at 4 °C until nematodes on all plates were measured using a stereo microscope (Leica M205 × C, 16 × magnification) for total body length (size), total number of offspring per recovered adult (reproduction), and for the number of pregnant nematodes (fertility), using a hand-held tally counter [41].

### 2.4. Monitoring in vivo ROS production response to ionizing radiation in C. elegans

While conventional redox-sensitive fluorogenic probes are non-specific, irreversible, and disruptive, genetically encoded fluorescent sensors can overcome such limitations [28,56]. Therefore, in the current study the *sod1::gfp* reporter strain and two ratiometric biosensors, *HyPer* and *Grx1-roGFP2*, were employed as *in vivo* proxies for ROS production following chronic exposure to gamma radiation [14,22]. Specifically, the *sod1::gfp* reporter strain was implemented to measure the expression of the cytosolic Superoxide dismutase 1, while the ratiometric biosensors *HyPer* and *Grx1-roGFP2* were adopted to measure the levels of $H_2O_2$ and the glutathione redox changes.

Treatments with Paraquat or $H_2O_2$ were used as positive controls for method validation for the *sod1::gfp* reporter strain and the *Grx1-roGFP2* ratiometric biosensor, respectively (Supporting material, Section S.M. 2-3.).

### 2.5. Epifluorescence microscopy

To analyse for changes in expression patterns following the exposure to ionizing gamma radiation, nematodes, exposed for 48 and 72 h from L1 stage, were transferred immediately onto an agar pad (2% agar) on a glass slide, immobilized with 30 mM of Sodium Azide (NaAzide), mounted and observed for the fluorescent signals.

Anatomical localization and intensity average of the fluorescent signal for *sod1::gfp* were assessed under a semi-automated research light microscope (Upright Microscope Leica DM6 B, 10X magnification) equipped with a 405 nm excitation and 535 nm emission filters for fluorescent intensity measurements (n = 10). For the ratio between the oxidized and reduced forms of either the *HyPer* or *Grx1-roGFP2* strains (n = 10), a second image, at excitation 490 nm and emission 535 nm, was taken. For each experiment, gain and exposure settings were kept unvaried between different treatments, in order to ensure comparable and unbiased measurements of the fluorescent signal. Intensity-normalized images of at least ten nematodes per treatment were taken

within 30 min from the sampling and quantification of the fluorescence signals was performed on the Leica® LAS software. A method validation with ROS inducer compounds (Paraquat and $H_2O_2$) was performed for the quantification of the fluorescent signal in *sod1::gfp* and *Grx1-roGFP2* (Supporting Material, sections S.M.2 and S.M.3). Gamma irradiation over 48 or 72 h induced decrease in *sod1::gfp* worm size in relation to controls, therefore fluorescence signals were normalized to the worms total body length. Oxidized/reduced *HyPer* and *Grx1-roGFP2* ratios were calculated as described by Back et al. [5].

### 2.6. Gene expression analysis

#### 2.6.1. Transcriptomic analysis

RNA sequencing was performed in order to obtain gene expression profiles of nematodes exposed to 0.4, 10.8 or 99.9 mGy $h^{-1}$ compared to control nematodes. For this purpose, after 72 h of exposure from L1 stage to young adult stage (n = 1000 per replicate, three biological replicates per treatment), nematodes were washed and snap-frozen in LIN (liquid nitrogen) and stored at -80 °C until used. Total RNA was extracted using Direct-zol Reagent (Nordic Biosite) and purified with RNeasy Mini Kit (Zymo Research) according to manufacture instruction. RNA purity and yield (A260/A280 > 1.8, A260/A230 > 2, yield > 100 ng/µl) was determined using NanoDrop-1000 Spectrophotometer (Thermo Scientific, Wilmington, DE) and quality (RIN > 7) was assessed with Agilent 2100 Bioanalyzer (Agilent Technologies, Palo Alto, CA) using RNA Nano LabChip Kit (Agilent Technologies). Photometric parameters and RNA integrity number determined the quality of the RNA sequenced samples. Strand-specific TruSeq™ RNA-seq pair-end libraries with 350 bp fragment size were prepared for each treatment (three biological replicates). For each sample ca $30x10^6$ reads (read length 150 bp) were sequenced using two lanes of Illumina HiSeq 4000 (Norwegian High Throughput Sequencing Centre, UiO Oslo, Norway), and made available on ArrayExpress with E-MTAB-8284.

Sequenced reads were mapped to the Ensemble reference genome WBcel235 using STAR [21]. Statistical analysis for detection of differentially expressed genes (DEGs) was done using Deseq2 package in the R software (rlog, variance Stabilizing Transformation) for transformed data [53], with FDR ≤0.05 and 0.3 ≤ log2fc ≤ -0.3 as cut off.

#### 2.6.2. Gene set enrichment analysis and phenotypical analysis

In order to obtain information about processes affected by gamma radiation with respect to anatomical, phenotypical and functional processes down to the single-cell level, the DEGs were subjected to gene ontology (GEA), tissue (TEA) and phenotype (PEA) Enrichment Analyses using the WormBase Enrichment tool (BioRxiv: https://doi.org/10.1101/106369) [2,48]. Analysis were performed using HyPergeometric probability distribution with Benjamini-Hochberg step-up algorithm FDR correction [3].

Moreover, a phenotypical analysis was performed by comparing the list of DEGs from the 100 mGy $h^{-1}$ exposure group with selected phenotypical variants using the public knowledge resource WormBase [48].

### 2.7. Statistical analysis

Results from somatic growth and reproduction assessment were analysed using the One-way Analysis of Variance (ANOVA) and when significance was found the Tukey *post hoc* test was adopted for comparison with the control group. Normality and homogeneity assumption were assessed on residuals by using Anderson-Darling normality test and visually on residuals vs. fitted value plot, respectively.

Fluorometric ratios from *HyPer* and *Grx1-roGFP2* and fluorescence intensity from *sod1::gfp* were used to measure levels of ROS in irradiated nematodes. Linear trends were estimated using Simple Linear Regression analysis (SLR) [57], while ANOVA and Tukey *post hoc* analysis were adopted for multiple comparisons with control treatment. Statistical analysis were performed using JMP Pro v14 (SAS institute, Cary, NC, USA) and SigmaPlot 10.0 (Systat Software, San Jose, CA).

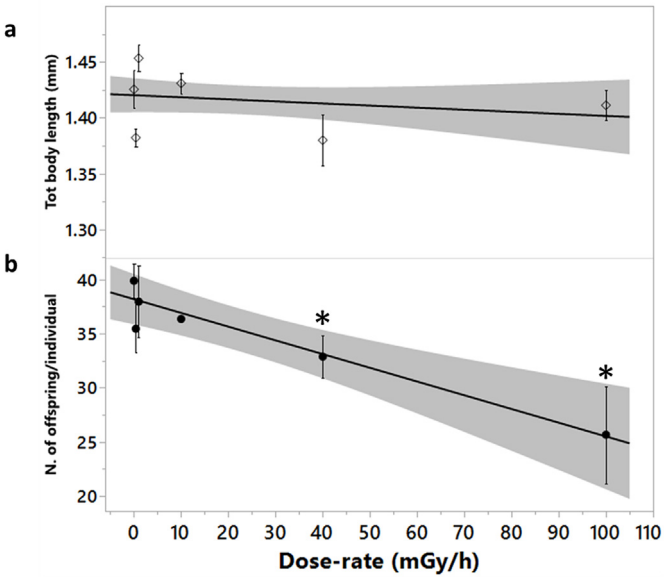


**Fig. 1.** Effects on **a)** Somatic growth and **b)** reproduction on wild-type *C. elegans* exposed to gamma radiation (mGy·$h^{-1}$, total doses in Table S8) for 96 h, in front row of 24-well plates containing MHRW/*E. coli* OP50 suspension. Data represents Mean ± SE (n = 15). Asterisks indicate significant difference to control treatment (Tukey post hoc, p-value < 0.05).

## 3. Results

### 3.1. Chronic gamma irradiation induced dose rate-dependent reprotoxic effect in C. elegans and no significant effects on somatic growth

In the nematode *Caenorhabditis elegans*, chronic exposure to gamma radiation did not induce any significant effect on lethality, morbidity, hatchability, or reproductive capacity at dose-rates ≤10 mGy $h^{-1}$ (total dose ≤1.4 Gy, Fig. 1b). Furthermore, non-significant effects on size/total body length were found in any of the wild-type irradiated groups compared to control nematodes (Fig. 1a).

However, after 96 h of exposure, a significant linear dose-dependent reduction (SLR, *p*-value < 0.001) in the number of offspring was shown with reproduction reduced by 20 and 40% (Tukey *post hoc*, *p*-value < 0.05) following exposure to 40 and 100 mGy $h^{-1}$, respectively (total doses ~3.9 and 9.6 Gy, Fig. 1b).

#### 3.1.1. Linear increase of sod-1 expression following chronic gamma irradiation

The effect of external whole body gamma irradiation on superoxide anion ($O_2^{\cdot-}$) metabolism was assessed *in vivo* using the superoxide dismutase *sod1::gfp* reporter strain [22]. In contrast to N2 strain, a minor but significant dose-dependent effect on somatic growth was shown when the *sod1::gfp* reporter strain was irradiated (SLR, *p*-value < 0.05), with a 10% reduction of the body length following 100 mGy $h^{-1}$ of gamma irradiation (total dose ~7.2 Gy, Tukey *post hoc*, *p*-value < 0.05) (Fig. S1).

Total body *sod-1* expression at 48 h of irradiation (≥1 mGy·$h^{-1}$) increased significantly in a dose-rate dependent manner (SLR, *p*-value < 0.0001) (Fig. 2a). The expression of *sod-1* also showed a time-dependent increase, since gamma radiation induced a significantly higher expression at 72 h of exposure in all treatments compared to 48 h and to non-irradiated nematodes (SLR, *p*-value < 0.0001). Moreover, One-Way ANOVA and Tukey *post hoc* tests showed a significant

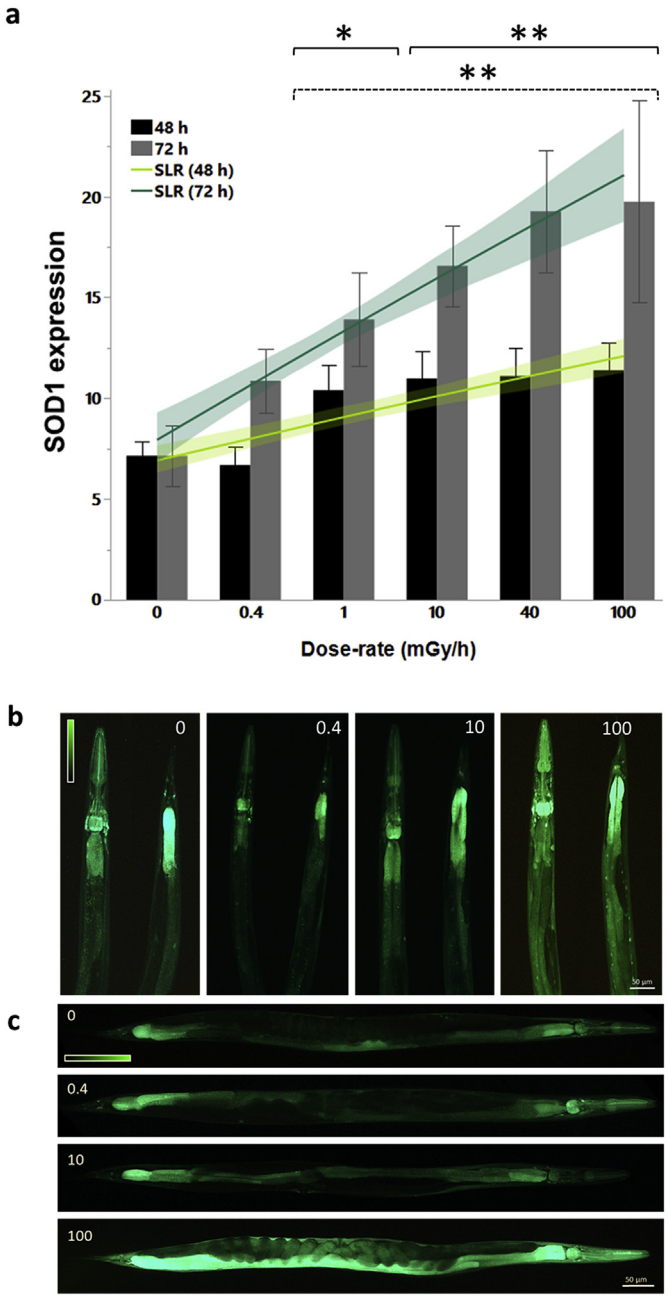


**Fig. 2.** **a**) Sod-1 expression assessed *in vivo* in *C. elegans* reporter strain *sod1::gfp*, after 48 and 72 h of exposure to increasing dose-rates of gamma radiation (mGy·h$^{-1}$, total doses in Table S8), in MHRW containing OP50. Data represent Mean ± 95% CI (n = 10), values are normalized to somatic growth. Dashed or continuous line with asterisk indicates significant difference to control treatment at 48 and 72 h, respectively (Tukey *post hoc*, *p*-value < 0.001 and < 0.0001). Projected on top of the bar chart are the regression lines for the SOD-1 expression on the $\log_{10}$(dose rate) values. **b**) Relative epifluorescence images of the expression pattern at different dose-rates of exposure (mGy·h$^{-1}$) after 48 (head and tail, respectively) and (**c**) 72 h of irradiation (tail to head orientation). Scale bar: 50 µm.

threshold-effect between 0.4 and 1 mGy·h$^{-1}$ (total dose between 0.02 and 0.05 Gy), with all exposure groups having a significantly higher expression of SOD1 compared to the control and 0.4 mGy·h$^{-1}$ treatments at both 48 or 72 h of exposure (*p*-value < 0.001 and < 0.0001) (Fig. 2a). The highest dose-rates of exposure in particular (40 and 100 mGy·h$^{-1}$), showed a 2-fold increase compared to the control group (Tukey *post hoc*, *p*-value < 0.0001) (Fig. 2a). Visually, this mark

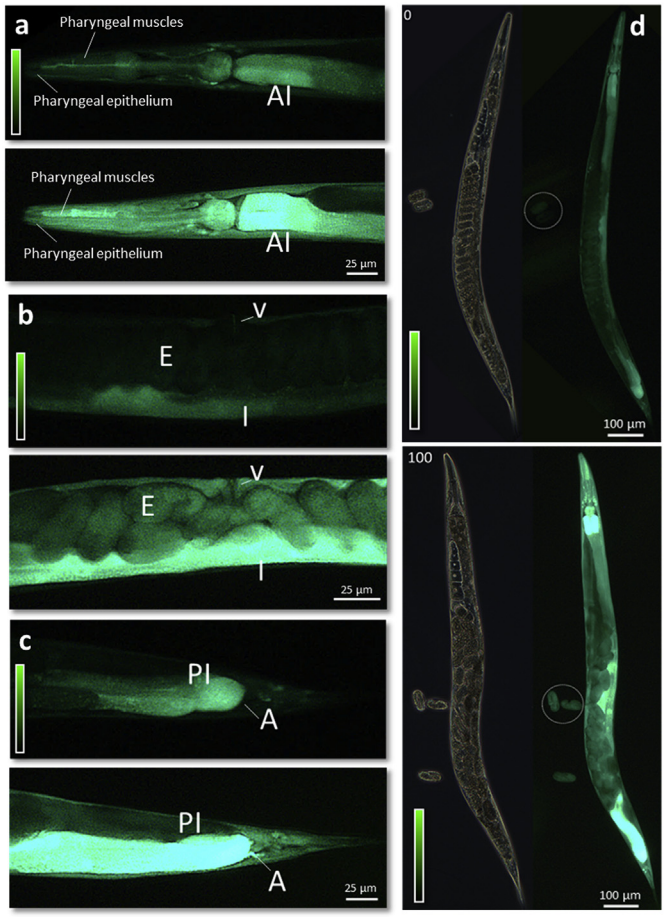


**Fig. 3.** Epifluorescence images of the expression pattern assessed *in vivo* in (**a**) pharynx (AI: anterior intestine); **b**) mid-body (E: embryos, V: vulva, I: intestine), and (**c**) tail (PI: posterior intestine, A: anus) of *C. elegans* reporter strain *sod1::gfp* after 72 h of irradiation to 0 (control) (**Top**) or 100 mGy h$^{-1}$ (total dose ~7.2 Gy, **Bottom**). **d**) Phase-Contrast optics and epifluorescence images of control (**Top**) nematodes or nematodes exposed to 100 mGy h$^{-1}$ (**Bottom**) for 72 h from L1 stage, white circle indicates laid embryos (from top to bottom, head to tail orientation). Scale bar: 25 or 100 µm.

increase was seen in nematodes' images, as shown in Fig. 2 b-c. Consistent with a previous study conducted by Doonan et al. [22], the signal from non-irradiated or low-dose exposed nematodes was primarily evident in the anterior and posterior part of the intestine, while at the highest dose-rate, the expression pattern was visible across the entire intestinal length for all the nematodes imaged after 48 or 72 h of exposure (Fig. 2b-c). Additionally, at 100 mGy·h$^{-1}$ (total dose ~7.2 Gy) in 40% of the assessed nematodes the fertilized embryos, both inside the uterus (in particular those in close proximity of the vulva) and the laid embryos exhibited enhanced fluorescent signal, while control embryos did not show any expression (Fig. 3b-d). Similarly, the vulva muscles along the body wall, together with the pharyngeal epithelium and muscles, the anterior/posterior intestine and the anus revealed a higher expression at 100 mGy·h$^{-1}$ (total dose ~7.2 Gy) in 50% of the imaged nematodes (n = 10, Fig. 3 a-b-c). The profound increase in *sod-1* expression in most parts of the nematodes' body is consistent with a model where the energy depositions and radical formation occurs uniformly in all irradiated cells, while the *sod-1:gfp* reporter is not equally effectively expressed in all tissues [22]. The fact that *sod-1* expression inevitably leads to $H_2O_2$ formation implied that further downstream effects on ROS metabolism might result from the irradiation.

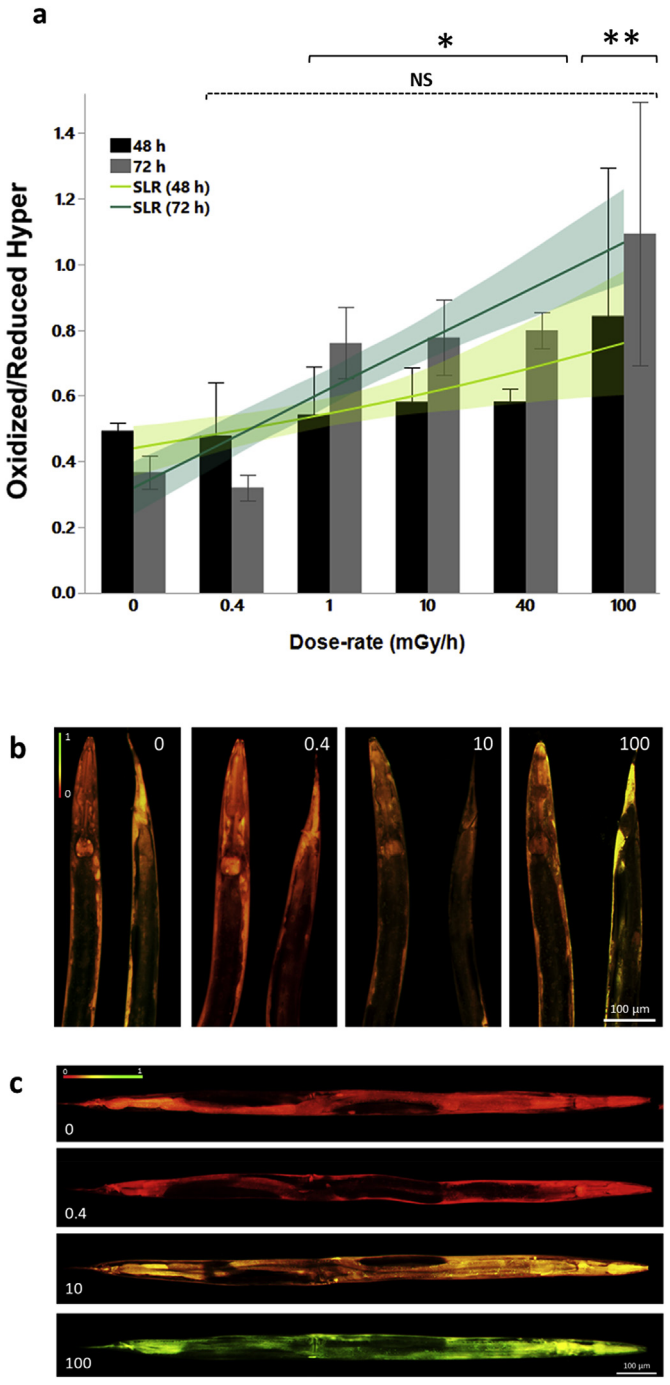


**Fig. 4.** **a**) $H_2O_2$ level assessed *in vivo*, in *C. elegans* ratiometric biosensor *HyPer*, after 48 and 72 h of exposure to gamma radiation (total doses in Table S8), in front row 24-well plates containing MHRW/OP50. Data represent Mean ± 95% CI (n = 10). Dashed or continuous line with asterisk indicates non-significant (NS) or significant difference to control treatment at 48 and 72 h, respectively (Tukey *post hoc*, *p*-value < 0.001 and < 0.0001). Projected on top of the bar chart are the regression lines for the $H_2O_2$ levels on the $\log_{10}$(dose rate) values. (**b**) Relative epifluorescence images of the $H_2O_2$ oxidation pattern at different dose-rates of exposure (mGy·h$^{-1}$) after (**b**) 48 (head and tail respectively) and (**c**) 72 h of irradiation (from left to right, tail to head orientation). Scale bar: 100 µm.

### 3.1.2. Dose-rate dependent increase in $H_2O_2$ production

The primary source of cellular $H_2O_2$ is via catalytic dismutation of $O_2^{\cdot-}$ by antioxidant enzymes including SOD1 [5]. The effects of gamma radiation on peroxide metabolism were investigated *in vivo* by using the *HyPer* biosensor [5]. At 48 h of exposure, analysis of the entire body of the nematodes showed that $H_2O_2$ levels increased linearly with dose-rate (SLR, *p*-value < 0.001) (Fig. 4a). At 100 mGy h$^{-1}$ (total dose ~4.8 Gy) the $H_2O_2$ levels were visibly increased (Fig. 4b), however, due to high inter-variability between organisms within the same treatment, this was not significant (Tukey *post hoc*, *p*-value > 0.05). Nonetheless, it was clear that the $H_2O_2$ levels increased with exposure time. At 72 h of irradiation, a significant dose-dependent increase (SLR, *p*-value < 0.0001) in the oxidized/reduced *HyPer* ratios was measured from doses ≥1 mGy h$^{-1}$ (Tukey *post hoc*, *p*-value < 0.001), as shown in Fig. 4 a. Consistent with the *sod-1* expression, the highest dose-rate (100 mGy·h$^{-1}$, total dose ~7.2 Gy) induced the highest levels of $H_2O_2$, either at 48 or 72 h (Tukey *post hoc*, *p*-value < 0.0001). This shows that gamma radiation at these dose-rates caused a significant peroxide production that surpassed the nematodes capacity to sequester $H_2O_2$. In contrast, both the control and 0.4 mGy·h$^{-1}$ groups showed a decreased $H_2O_2$-level between 48 and 72 h of exposure.

Accordingly, when assessing the accumulation of hydrogen peroxide in different tissues at 48 h, it was evident that no visible oxidation pattern was identified with no evident change observed in the fluorescence ratio below 100 mGy·h$^{-1}$ (total dose < 7.2 Gy, Fig. 4b), while after 72 h of exposure, at ≥10 mGy·h$^{-1}$ the nematodes showed a significant enhanced level of oxidation (Fig. 4c). Moreover, the *HyPer* oxidation pattern showed a visible dose-dependent increase, from a reduced signal observed in the control and 0.4 mGy·h$^{-1}$ groups, to an oxidized signal in the 10 and 100 mGy·h$^{-1}$ groups (Fig. 4 c, total doses in Table S8). In order to investigate whether there were differences between certain tissues or cell types, the *HyPer* ratios were quantified in the Pharynx posterior bulb and in the Posterior intestine after exposure to 100 mGy·h$^{-1}$ compared to non-irradiated nematodes (Fig. 5 a-b-c). Consistent with the whole-body measurements (Fig. 4a and 5 a), the 100 mGy·h$^{-1}$ exposure (total dose ~7.2 Gy) showed a significant difference in the oxidation signal (green fluorescent signal) compared to controls, specifically in the pharynx and along the posterior part of the intestine (Student's t-test, *p*-value < 0.0001) (Fig. 5). The results did however not reveal any difference between different tissues or cell types (Student's t-test, *p*-value > 0.05).

### 3.1.3. Glutathione redox changes

The glutathione disulphide-glutathione couple [GSSG]/[2GSH] serves as the cell's primary mediator for the maintenance of redox homeostasis [5]. Therefore, the oxidized to reduced ratio [GSSG]/[2GSH] of *Grx1-roGFP2* [5] was used as a proxy to assess the impact of chronic exposure to ionizing radiation *in vivo* on the redox potential and to visualize the relative oxidation pattern in the nematode *C. elegans*. At 48 h from L1 stage, at dose-rates as low as 0.4 mGy h$^{-1}$ (total dose ~0.02 Gy), a significant imbalance between oxidized to reduced signal was measured on the irradiated *Grx1-roGFP2* compared to control nematodes (Tukey *post hoc*, *p*-value < 0.001) (Fig. 6a). This significant oxidative imbalance was shown for all measured dose-rates (Tukey *post hoc*, *p*-value < 0.001). Despite the statistically significant imbalance detected on the whole-body measurements after 48 h of exposure, in all the irradiated groups, we found no evidence of tissue-specific effect compared to control nematodes (Fig. 6b).

In contrast, at 72 h of exposure, assessment of oxidative effects on whole body was hampered by excessively large variation between individuals (S.M.4, Fig. S4a-b). However, previous reports have demonstrated large differences between tissues [5]. At this time-point, the only dose-rate inducing a higher but not statistically significant oxidation of the [GSSG]/[2GSH] couple was 100 mGy h$^{-1}$ (total dose ~7.2 Gy) (Tukey *post hoc*, *p*-value > 0.05) (Fig. 6a), we therefore, investigated effects on different tissues and cell types in this exposure group compared to control nematodes. This analysis showed a significant oxidation in the gonads compared to the control (Student's t-test, *p*-value < 0.001) (Fig. 7b-c), while the signal measured in the spermatheca showed no difference between these two groups (Student's

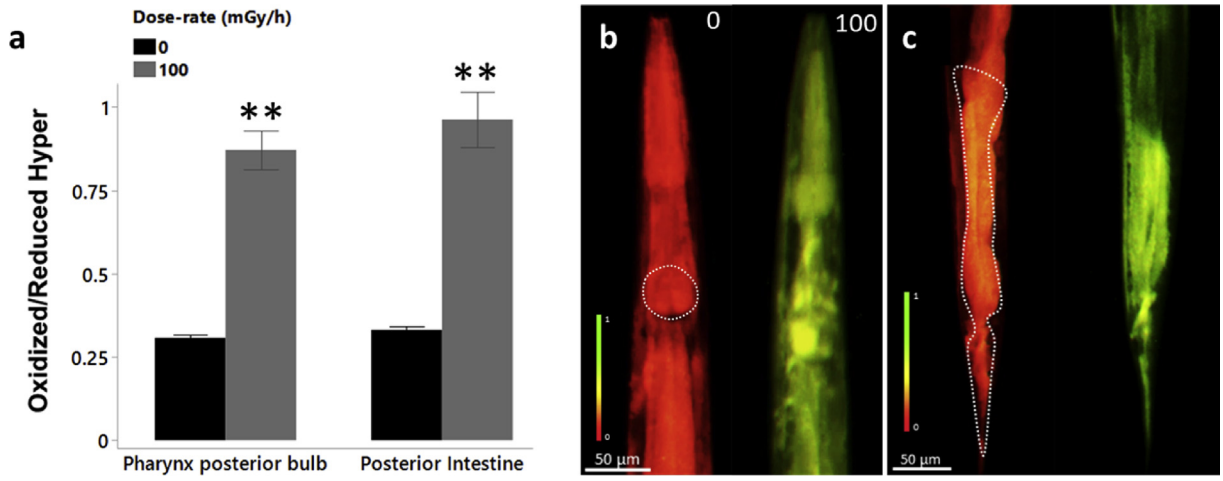


**Fig. 5. a**) $H_2O_2$ level assessed *in vivo* in specific tissues of *C. elegans* ratiometric biosensor *HyPer*, after 72 h of exposure to 0 and 100 mGy $h^{-1}$ (total dose ~7.2 Gy) of gamma radiation. Asterisk indicates significant difference to control treatment (Student's *t*-test, *p*-value < 0.0001). (**b**) Epifluorescence images of the relative expression pattern assessed *in vivo* in (**b**) the pharynx posterior bulb and (**c**) posterior intestine of *C. elegans* biosensor *HyPer* after 72 h of irradiation to 0 (control) or 100 mGy $h^{-1}$. Scale bar: 50 µm.

t-test, *p*-value > 0.05) (Fig. 7c-d).

### 3.2. Chronic exposure to gamma radiation induces dose-rate dependent effects on C. elegans transcriptome

A gene expression analysis was performed after 72 h of exposure to gamma radiation from L1 stage in order to identify potential changes in the nematode's transcriptional program. The RNA-seq analysis revealed a clear dose-dependent increase in the number of differentially expressed genes (DEGs) (Fig. S5a). No significant differences in the gene expression profile were found in nematodes exposed to 0.4 mGy $h^{-1}$ compared to the control group, while the 10 and 100 mGy $h^{-1}$ groups (total doses ~0.8 and 7.2 Gy) showed a total of 62 and 1317 DEGs, respectively, with 15 DEGs in common between these two treatments (Fig. S5 b and Table S1). The complete list of DEGs resulting from 10 and 100 mGy $h^{-1}$ exposure groups can be found in Supplementary Tables S2 and S3, respectively.

#### 3.2.1. Functional enrichment analysis of DEGs

A gene set enrichment analysis was performed on the DEGs resulting from 10 and 100 mGy $h^{-1}$ exposure groups in order to identify functions significantly affected by exposure to gamma radiation with respect to tissue, phenotype and gene ontology (Fig. S6-7, Tables 1 and 2, Table S6). A clear distinction between the expression profiles was found in the DEGs resulting from the two exposure groups (Fig. S5). The exposure to 10 mGy $h^{-1}$ (total dose ~0.8) indicated overall effects on functions related to intestine, immune, reproductive and nervous systems (Fig. S6 a-b-c).

When the same analysis was performed on 100 mGy $h^{-1}$ DEGs, several functions and categories related to reproduction and effects on progeny were significantly enriched among down-regulated genes. Specifically, the reproductive system, embryonic development, meiotic chromosome segregation and cell cycle, spindle defective in early embryo, aneuploidy and embryonic cell physiology were among the most over-represented functions and variants observed (Fig. S7 a-b-c, Table S4). The TEA tool identified more than 300 down-regulated genes related to the reproductive system and more than 100 genes related to the

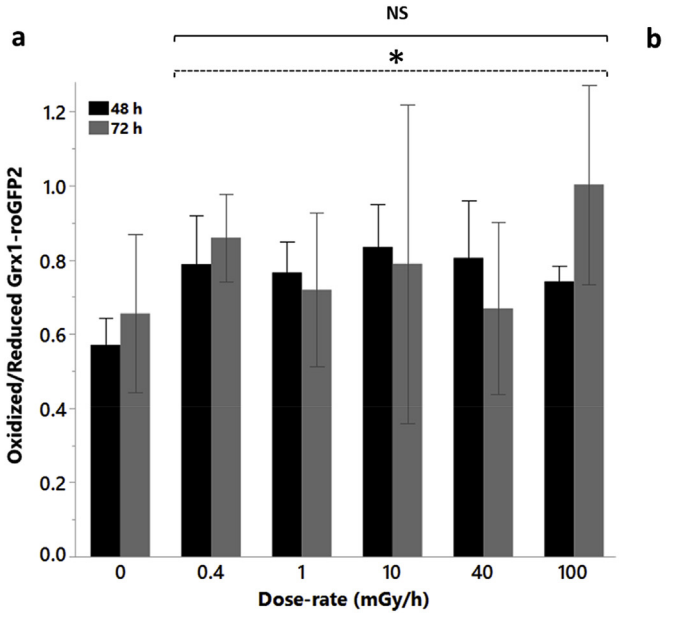


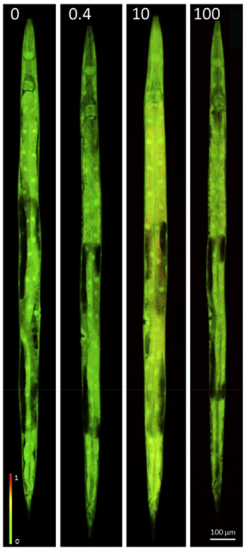


**Fig. 6. a**) *In vivo* measurement of oxidized to reduced ratio of the *C. elegans* ratiometric biosensor *Grx1-roGFP2*, assessed after 48 and 72 h of exposure to gamma radiation (total doses in Table S8), in front row 24-well plates containing MHRW/OP50. Data represent Mean ± 95% CI (n = 10). Dashed or continuous line indicates non-significant (NS) or significant difference (asterisk) to control treatment at 48 and 72 h, respectively (Tukey *post hoc*, *p*-value < 0.001). (**b**) Relative epifluorescence images of the oxidation pattern in *Grx1-roGFP2* at different dose-rates of exposure (mGy·$h^{-1}$) after 48 h of irradiation (from top to bottom, head to tail orientation). Scale bar: 100 µm.

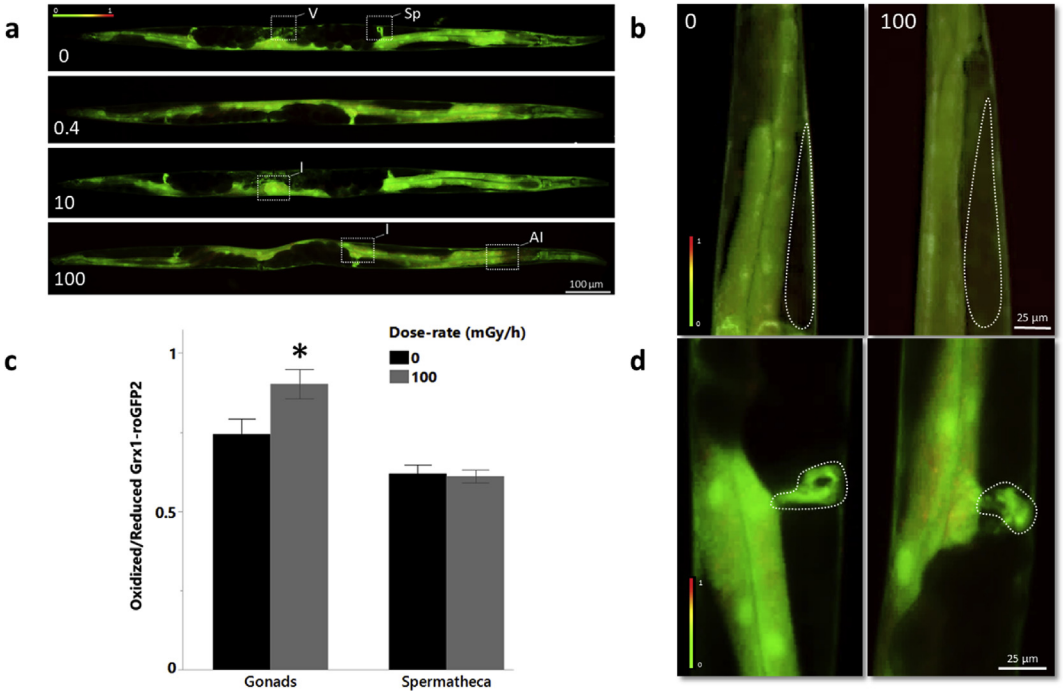


**Fig. 7. a**) Epifluorescence images of the oxidation pattern in *Grx1-roGFP2* after 72 h of gamma irradiation to different dose-rates of exposure (mGy·h$^{-1}$, total doses in Table S8) in the entire body (V: vulva, Sp: spermatheca, I: intestine, AI: Anterior Intestine) (from left to right, tail to head orientation) or in selected tissues **b**) gonad and **d**) spermatheca. (**c**) Relative measurement of the GSSG/2GSH ratio in gonad and spermatheca after exposure to 0 (control) or 100 mGy h$^{-1}$ of gamma radiation. Asterisk indicates significant difference to control treatment (Student's *t*-test, *p*-value $<$ 0.001). Scale bar: 25 or 100 µm.

muscular system (Fig. S7 c, Table S4). From the muscular system category, 19 genes had mitochondrial functions, including mitochondrial ribosomal proteins (*mrpl* and *mrps*), genes involved in mitochondrial membrane and genome maintenance (*pgs-1*, *R04F11.5*, *tomm-7*, *C27H6.9* and *rpap-3*) and mitochondrial dysfunction or disease (F39H2.3, nuaf-1 and pgs-1) (Table S4). The Embryonic development variant identified by the PEA tool, on the other hand, included 94 down-regulated genes, among these, genes required for meiotic and mitotic chromosome segregation (*mut-2*, *dnc-2*, *him-10*, *nmat-2*, *cec-3*, *syp-3*, *rsa-1*, *unc-59*, *cids-1*, *him-8*, *nos-2*, *hpo-9* and *hus-1*), apoptosis and DNA repair (*rad-54*, *ced-12*, *pch-2*, *tyms-1*, *uri-1*), gamete development and fertilization (*trcs-1*, *nos-2*, *unc-59*, *pgs-1*, *uri-1*, *spd-3*, *hus-1 and mdt-6*) (Table S4). The genes *mut-2*, *hus-1*, *nos-2*, *him-10*, *cids-1*, *syp-3*, *rsa-1* and *him-8* are all related to adverse 'variant Aneuploidy', 'Chromosome segregation', 'Meiotic cell-cycle functions' and the 'Reproductive system' (Table S4).

Similarly, the up-regulated genes resulting from the same exposure group showed that important functions with respect to cellular development, post-embryonic development, cuticle and collagen synthesis, sex organ, protein interaction and cytokinesis were affected (Tables 1 and 2, Table S6). The GEA tool identified multiple molecular functions related to the modulation of gene expression via transcriptional initiation, post-transcriptional modification and RNA transport and processing (Table 1, Table S5). Also chromatin remodelling appeared to be affected as evidenced by 'Protein heterodimerization activity' category, which included 31 core histones (Table 1, Table S5). The most significantly enriched PEA category comprised 24 up-regulated genes related to 'Variant Sister Chromatid segregation defective in early embryo' (q-value $<$ 0.00001) (Table 2, Table S5). Further indication of effects related to cell division and reproduction were seen by 19 histones and ribosomal subunits encoding genes associated to 'Diplotene absent during oogenesis' phenotype. Another 19 up-regulated genes were related to 'Apoptosis fails to occur'. These included activator of the programmed cell-death pathway, *egl-1*, regulator of asymmetric cell division, *ces-2*, regulator of cell fate during post-embryonic development, *mab-5*, *mcd-1*, which promotes the developmentally programmed progression of cells through apoptosis and 7 genes encoding for large and small ribosomal subunits (*rpl* and *rps*) (Table S5). Collectively, a large proportion of the DEGs were related to cell cycle impairments and responses to genotoxic effects.

### 3.2.2. *Over-represented categories modulated by ionizing radiation-induced oxidative damage*

The transcriptome analysis, at 100 mGy h$^{-1}$, identified several genes involved in oxidation-reduction processes and AOD (antioxidant defence) system, within the cytosol or in the mitochondrion (*ctl-1*, *COX1*, *COX2*, *COX3*, *cox-4*, *cox-5B*, *cox-6C*, *cox-7C*, *CYTB*, *hpo-19*, *sdhd-1*, *ucr-2.1*, *gst-20*, *egl-1*, *egl-18*, *trx-2*, *trxr-2*, *sod-1* and *rad-8)*. Moreover, we found significant up-regulation of genes involved in the glutathione *de novo* synthesis, such as F22F7.7 and gln-3. Therefore, in order to identify specific transcriptional responses related to the increased generation of ROS and evidence of oxidative damage effects on cell physiology and metabolism, we performed an in depth manual assignment of the DEGs from nematodes exposed to 100 mGy h$^{-1}$ into relevant categories assigned from the curated WormBase phenotype [48] and transcriptomic analysis of oxidative stress [66] (Fig. 8, Table S7). As expected, a number of genes within Oxidative stress response, PCD (Programmed Cell Death), DNA damage and response to ionizing radiation were found (Fig. 8). Within the first most over-represented category (Programmed cell death), we found genes related to general response to stress, such as Autophagy (*atg-3*, *atg-9*, *ces-2* and *rab-7*), but also Cell cycle and Cell division (*pch-2*, *egl-1*, *hus-1*, *ced-12*, *dapk-1*, *ces-2*, *chk-1*, *mcd-1*, *tads-1*, *pcn-1*, *car-1*, *set-17*), Ribosomal proteins (*rpl-12*, *rpl-13*, *rpl-18*, *rpl-19*, *rpl-20*, *rpl-26*, *rps-10*, *rps-20*, *rps-26*, *rps-3*, *rps-6*, *rps-9*), Proteasome (*pbs-1*, *pbs-1*, *pbs-5*) and Histones (*his-24*, *his-68*, *his-3*, *his-7*, *his-61*, *his-47*) (Table S7). Phenotypes directly related to exposure to ionizing radiation were also found with respect to organismal and germline response, these included genes related to cell cycle and DNA repair (*rad-54*, *chk-1*, *hus-1*, *umps-1 and rpa-2*), innate immune response (*elt-2*), chromosome segregation and apoptosis (*hus-1*, *rad-54*,

**Table 1**
Over-represented biological processes, molecular functions and cellular components functional categories, from Gene Ontology (GO), which were up-regulated in *C. elegans* after 72 h of exposure to 100 mGy $h^{-1}$ of gamma radiation. HyPergeometric probability distribution is adopted to measure the number of enriched terms (Observed number of DEGs in each specific function).

| Term (GEA) | Observed | Enrichment Fold Change | P value | Q value |
|---|---|---|---|---|
| Intracellular GO:0005622 | 466 | 1.1 | 0.0053 | 0.023 |
| Organelle GO:0043226 | 401 | 1.1 | 0.0019 | 0.011 |
| Cytoplasm GO:0005737 | 295 | 1.1 | 0.016 | 0.061 |
| Cellular developmental process GO:0048869 | 92 | 1.7 | 5.90E-07 | 9.40E-06 |
| Regulation of nucleobase-containing compound metabolic process GO:0019219 | 91 | 1.2 | 0.015 | 0.061 |
| Membrane-enclosed lumen GO:0031974 | 86 | 1.3 | 0.0026 | 0.013 |
| Supramolecular complex GO:0099080 | 61 | 2.7 | 1.90E-13 | 6.10E-12 |
| Cytoskeleton GO:0005856 | 60 | 1.8 | 6.50E-06 | 6.90E-05 |
| Hydrolase activity acting on acid anhydrides GO:0016817 | 57 | 1.3 | 0.027 | 0.087 |
| Structural constituent of cuticle GO:0042302 | 53 | 4.4 | 1.10E-21 | 1.50E-19 |
| Post-embryonic development GO:0009791 | 53 | 1.5 | 0.0015 | 0.0093 |
| Collagen trimer GO:0005581 | 49 | 4 | 3.20E-18 | 2.10E-16 |
| Peptide biosynthetic process GO:0043043 | 48 | 1.8 | 2.00E-05 | 0.0002 |
| Neurogenesis GO:0022008 | 44 | 2.3 | 1.10E-07 | 2.40E-06 |
| Neuron development GO:0048666 | 39 | 2.5 | 2.50E-08 | 6.30E-07 |
| Cell projection organization GO:0030030 | 39 | 1.8 | 8.10E-05 | 0.00074 |
| Protein heterodimerization activity GO:0046982 | 35 | 4.6 | 9.40E-16 | 4.00E-14 |
| Nucleoplasm GO:0005654 | 33 | 1.6 | 0.0024 | 0.013 |
| Actin filament-based process GO:0030029 | 31 | 2.7 | 1.30E-07 | 2.40E-06 |
| Cell part morphogenesis GO:0032990 | 30 | 2.5 | 7.40E-07 | 1.10E-05 |
| Nucleoside phosphate metabolic process GO:0006753 | 30 | 1.4 | 0.02 | 0.07 |
| Ribose phosphate metabolic process GO:0019693 | 29 | 1.7 | 0.0012 | 0.0083 |
| Cell morphogenesis involved in differentiation GO:0000904 | 28 | 2.5 | 3.10E-06 | 3.60E-05 |
| Purine nucleotide metabolic process GO:0006163 | 28 | 1.8 | 0.00066 | 0.0048 |
| Neuron projection guidance GO:0097485 | 24 | 2.8 | 8.00E-07 | 1.10E-05 |
| Regulatory region nucleic acid binding GO:0001067 | 24 | 1.8 | 0.0014 | 0.0093 |
| Post-embryonic animal organ development GO:0048569 | 22 | 1.7 | 0.0041 | 0.019 |
| Negative regulation of RNA metabolic process GO:0051253 | 22 | 1.5 | 0.018 | 0.063 |
| Purine nucleoside monophosphate metabolic process GO:0000976 | 21 | 2.3 | 8.40E-05 | 0.00074 |
| Structural constituent of ribosome GO:0003735 | 21 | 2.1 | 0.00043 | 0.0035 |
| Transcription regulatory region sequence-specific DNA binding GO:0000976 | 20 | 1.9 | 0.0018 | 0.011 |
| RNA splicing via transesterification reactions GO:0000375 | 18 | 2.2 | 0.00064 | 0.0048 |
| RNA polymerase II regulatory region DNA binding GO:0001012 | 17 | 1.8 | 0.0066 | 0.028 |
| Reproductive system development GO:0061458 | 17 | 1.8 | 0.0071 | 0.029 |
| Development of primary sexual characteristics GO:0045137 | 16 | 2 | 0.0028 | 0.014 |
| Regulation of cellular amide metabolic process GO:0034248 | 16 | 2 | 0.0031 | 0.015 |
| Molting cycle GO:0042303 | 14 | 1.7 | 0.016 | 0.061 |
| Negative regulation of transcription by RNA polymerase II GO:0000122 | 14 | 1.7 | 0.017 | 0.063 |
| Small ATPase binding GO:0031267 | 13 | 1.7 | 0.025 | 0.083 |
| Ribonucleoprotein granule GO:0035770 | 12 | 1.7 | 0.024 | 0.082 |

*ing-3*, *lin-40* and *car-1*).

From the total DEGs resulting after exposure to 100 mGy $h^{-1}$ we found 40 genes involved in mitochondrial functions, among them, genes related to mitochondrial membrane, mitochondrial ribosomal proteins, mitochondrial metabolism and mitochondrial respiratory chain. Among the selected phenotypes, mitochondrial metabolism included mostly up-regulated genes, while mitochondrial respiratory chain was the only phenotype significantly down-regulated, comprising 10 (*COX1*, *COX2*, *COX3*, *ND1*, *ND2*, *ND3*, *ND4*, *ND5*, *CYTB* and *ATP6*) of the 12 genes which encode for the oxidative phosphorylation system [17] (Table S7).

The second most represented category (Fig. 8) included 85 genes found in common with RNA sequencing analysis performed on oxidative stressed wild-type N2 (499 DEGs in total) after exposure to

**Table 2**
Functional over-represented variants from Phenotype Enrichment analysis (PEA) that were up-regulated in *C. elegans* after 72 h of exposure to 100 mGy $h^{-1}$ of gamma radiation (total doses ~7.2 Gy). Hypergeometric probability distribution is adopted to measure the number of enriched terms (Observed number of DEGs in each specific function).

| Term (PEA) | Observed | Enrichment Fold Change | P value | Q value |
|---|---|---|---|---|
| Protein interaction variant WBPhenotype:0001369 | 71 | 1.3 | 0.0053 | 0.09 |
| Avoids bacterial lawn WBPhenotype:0000402 | 65 | 1.6 | 4.20E-05 | 0.0046 |
| Cytokinesis variant WBPhenotype:0002408 | 48 | 1.7 | 6.40E-05 | 0.0047 |
| Endosome morphology variant WBPhenotype:0002090 | 45 | 1.5 | 0.0028 | 0.055 |
| Lysosome-related organelle morphology variant WBPhenotype:0002095 | 42 | 1.5 | 0.0024 | 0.054 |
| Neuronal outgrowth variant WBPhenotype:0000572 | 38 | 1.7 | 0.00051 | 0.023 |
| Sluggish WBPhenotype:0000646 | 34 | 1.6 | 0.0015 | 0.049 |
| Endosome localization variant WBPhenotype:0002100 | 34 | 1.7 | 0.00088 | 0.032 |
| Sister chromatid segregation defective early emb WBPhenotype:0000772 | 26 | 3.1 | 2.40E-08 | 5.20E-06 |
| Pleiotropic defects severe early emb WBPhenotype:0000270 | 22 | 2 | 0.00037 | 0.02 |
| Diplotene absent during oogenesis WBPhenotype:0001954 | 19 | 1.9 | 0.0016 | 0.049 |
| Apoptosis fails to occur WBPhenotype:0000184 | 16 | 1.9 | 0.0035 | 0.063 |
| Gonad small WBPhenotype:0001957 | 15 | 2.1 | 0.0022 | 0.053 |

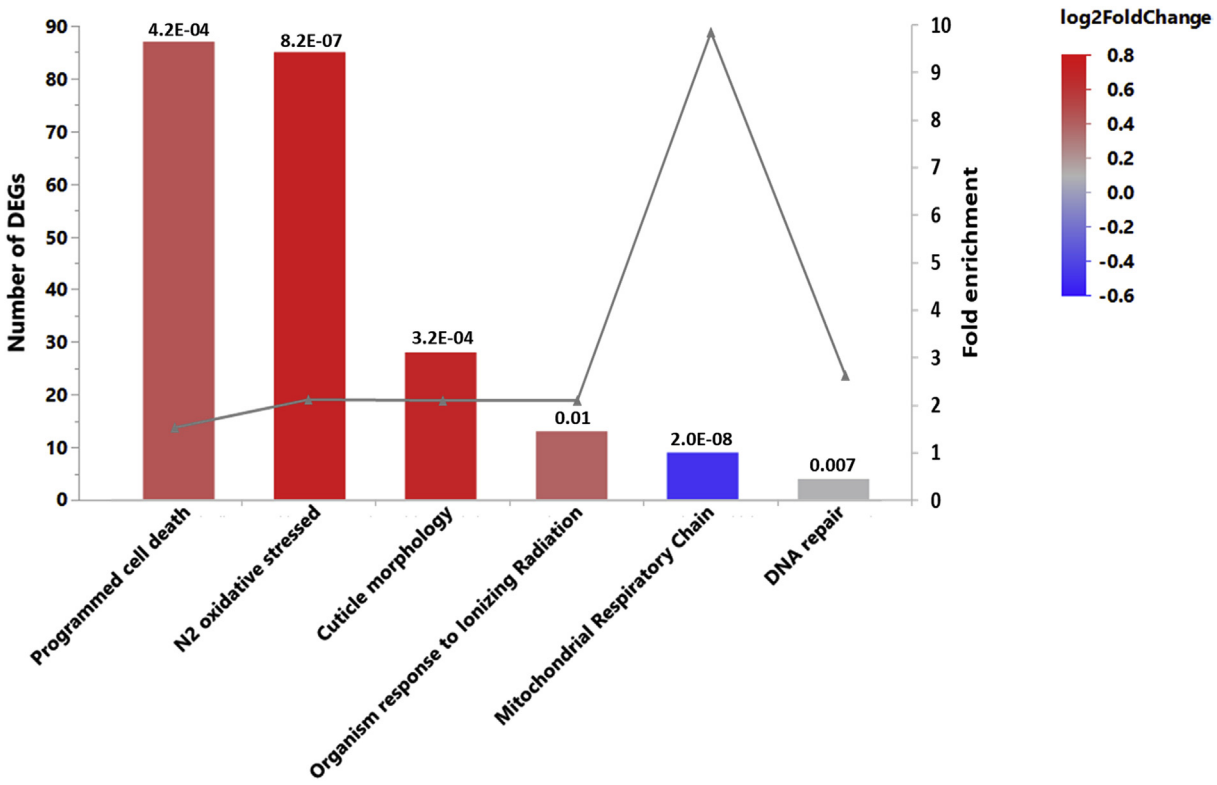


**Fig. 8.** Over-represented categories modulated by ionizing radiation-induced oxidative damage resulting from 72 h exposure to 100 mGy $h^{-1}$ of gamma radiation (total doses ~ 7.2 Gy) in the nematode *C. elegans*. (Data labels indicate Fisher's exact test *p*-values).

Paraquat from a previous study by Shin et al. [66]. Among these DEGs found in common, 80 genes showed significant up-regulation and were mostly related to Collagen (*col-104*, *col-107*, *col-109*, *col-130*, *col-155*, *col-166*, *col-167*, *col-48*, *col-77*, *col-81*, *col-95*, *let-2*), Mitochondrion (*sdhd-1*, *tomm-7*, *F58F12.1*), Histones (*his*) and Ribosomal proteins (*rpl*, *rps*), the list also included the heat-shock protein *hsp-3* and the *daf-2* regulated gene *dao-2*.

Consistent with the effects induced by oxidative damage [66], lipid metabolism, cuticle morphology, protein degradation and energy expenditure were also among the most over-represented phenotypes, comprising mostly up-regulated genes (Table S7).

## 4. Discussion

The oxidative damage exerted on cellular molecules and macromolecules accounts for the total indirect effect following exposure to ionizing radiation [4,62]. Therefore, the assessment of ROS/AOD levels and the subsequent oxidative damage response represents a fundamental parameter to understand and monitor the changes in the homeostasis of an organism. To the best of our knowledge, this is the first study to demonstrate *in vivo* ROS formation, antioxidant response and oxidative stress effects to the cellular redox homeostasis in a radiation tolerant organism subjected to chronic gamma irradiation. Furthermore, we connect molecular initiating events related to ROS production and redox imbalance to phenotypical effects by performing a deep gene expression analysis. Consistent with previous studies [13,55], only dose-rates ≥40 mGy $h^{-1}$ (total doses ≥3.9 Gy) were able to inflict a reprotoxic effect (Fig. 1). In line with studies performed on other aquatic and soil organisms [29,30,81], our study suggests that ROS production plays an important role in the induction of molecular, cellular and organismal adverse effects also in *C. elegans*, with reproduction being the most radiosensitive endpoint compared to somatic growth, fertility and mortality [1,36,40,59]. No significant effects with respect to somatic growth or somatic cell viability could be detected even for nematodes that received 100 mGy $h^{-1}$ (total doses ~9.6 Gy) during their entire larval development. This demonstrates that *C. elegans* has a relatively high tolerance towards the effects of gamma radiation at the organismal level, but the mechanisms involved remained to be elucidated. By using ROS reporter strain we were able to investigate whether ionizing radiation affected cellular ROS metabolism in *C. elegans in vivo*, but also to address whether tolerance to ionizing radiation is mediated by high anti-oxidant capacity.

### 4.1. ROS production and scavenging in C. elegans exposed to chronic gamma radiation

External gamma irradiation causes ionizations homogenously in the whole body of an organism like *C. elegans*. We therefore hypothesised that ROS formation would be dose-rate dependent and uniform within all cells and tissues of the nematode. To investigate the effect of gamma radiation on ROS formation in *C. elegans* we first assessed the effect on *sod-1* gene expression as a proxy for $O_2^{\cdot-}$ production. The results confirmed an overall linear correlation between dose-rate and *sod-1* expression (Fig. 2). The response was uniform throughout the entire nematode body, including embryos (Fig. 2c and 3 d). Any discrepancies could be ascribed to tissue specific constraints *of sod-1::gfp* expression [22]. The fact that *sod-1* expression increased with time implies continuous formation and accumulation of $O_2^{\cdot-}$ during the exposure. These observations are consistent with the LET-model for radiolysis radical formation [68]. Notably, the $O_2^{\cdot-}$ formation by gamma radiation appears to be quite high considering that the *sod-1* response was about 3-fold higher compared to Paraquat exposure (Fig. S2). This indicated a considerable potential for other effects of ROS and oxidative damage.

In other species (i.e. bdelloid rotifers) the enhanced capacity for scavenging reactive molecular species generated by ionizing radiation has been addressed as one of the major contributors to radiation resistance [46]. Therefore, in the current study, we have assessed the redox status after chronic irradiation, in order to verify whether the

unusually high abundance of AODs in *C. elegans* compared to other organisms plays a key role in its tolerance towards ionizing radiation.

Consistent with results from other organisms expressing high radioresistance [46], we measured higher levels of AODs in nematodes exposed to much lower dose-rates of gamma radiation. In particular, after 48 h of exposure and from dose-rates higher than 1 mGy $h^{-1}$ (total doses ≥0.05 Gy), we measured a linear dose-rate dependent increase of cytosolic superoxide dismutase and a significant imbalance in the oxidation of the [GSSG]/[2GSH] couple (Fig. 2 a and 6. a). On the other hand, at this time-point, $H_2O_2$ levels did not show a significant change in any of the irradiated groups, even though a linear dose-dependent increase was detected (SLR) (Fig. 4 a). A time-dependent increase in the levels of SOD1 and $H_2O_2$ was measured after 72 h of irradiation, with SOD1 and $H_2O_2$ levels being significantly increased already at dose-rates ≥1 mGy $h^{-1}$ (total doses ≥0.08 Gy). At this time-point, as should be expected, the highest dose-rate of exposure (100 mGy $h^{-1}$, total dose ~7.2 Gy) showed the most elevated levels of ROS and AODs (Fig. 2 a, 4. a, 6. a).

Under 'normal' aerobic conditions, during mitochondrial respiration, approximately 2–3% of oxygen is incompletely reduced and leads to the production of a small amount of superoxide radical anion ($O_2^{\cdot-}$) through the mitochondrial electron transport chain (ETC) [75]. This free radical is transformed into hydrogen peroxide ($H_2O_2$), which is also a potent oxidizing agent, by the mitochondrial isoforms SOD2 and SOD3 (manganese superoxide dismutase) [9,12,18,23]. Nevertheless, $O_2^{\cdot-}$ may also leak into the cytosol through the voltage-dependent anion channels [33] to become the substrate for the cytosolic Cu, Zn-SOD (SOD1).

Upon cell exposure to ionizing radiation, the physiological production of ROS in the different compartments of the cell are joined by ROS produced by water radiolysis [71]. Moreover, perturbation in the redox balance can be further affected when mitochondrial dysfunction occurs in irradiated cell, leading to ulterior production of mitochondrial ROS in addition to the radicals resulting from the water radiolysis [4].

Therefore, we suggest that chronic exposure to gamma radiation may induce the accumulation of $O_2^{\cdot-}$inside the mitochondria, which due to the increased leakage of $O_2^{\cdot-}$ in the cytosol contributed to the increased *sod-1* expression (Fig. 2a). Moreover, the dismutation of $O_2^{\cdot-}$ and the consequently increased production of $H_2O_2$ (Fig. 4a) and other ROS, over time, culminated in the observed effect on the redox status (Fig. 6a, 7b). Maintenance of the proper [GSSG]/[2GSH] ratio ensures redox homeostasis, whereas changes to this ratio provides effective means to adjust the redox state between as well as within cellular compartments under different physiological conditions [42]. The significant changes in the ratio of reduced glutathione to glutathione disulphide in the different tissues and cell compartments (Figs. 6 and 7 b-c) indicated that ROS were produced at higher rates than *C. elegans* was able to sequester. Furthermore, the increased ROS production did significantly affect the overall cellular redox balance at 48 h of exposure (Fig. 6a). It appears that at 72 h of exposure the nematodes mobilized AOD systems were capable of counteracting the redox imbalance in most tissues (Fig. 7a) despite the increased ROS levels (Fig. 2 a and Fig. 4a).

Glutathione plays an essential role in the antioxidant defence system, as a source of electrons for antioxidant enzymes such as glutaredoxins and peroxidases [60]. Two possible events can explain the partial restored balance of glutathione, observed after 72 h of exposure: i) the high concentrations (1–11 mM) of glutathione in the cell, which ensure an abundance of electrons for these antioxidant systems and thus a robust buffer against oxidative shifts in the redox state [65]; ii) the induced glutathione *de novo* synthesis, as indicated by the up-regulation of gamma-glutamylcyclotransferase (*F22F7.7*) and glutamine synthetase (*gln-3*) [54], resulting from RNA-seq analysis on nematodes exposed to 100 mGy $h^{-1}$ (total dose ~7.2 Gy) (Table S3).

However, changing the redox balance can alter the physiological homeostasis of an organism not only because ROS are harmful for proteins, lipids and nucleic acids, but also because they represent important signalling molecules in a biological system, and even a minor change can result in a substantial alteration for example in terms of metabolism, cell proliferation and host defence [26]. Despite the partially restored redox balance, observed after 72 h with the *Grx1-roGFP2* strain, the increased expression of SOD1 and the high $H_2O_2$ levels measured, together with the glutathione redox imbalanced, observed after 48 h of chronic gamma irradiation and in the gonads of 72 h irradiated nematodes, implied that the changes of the redox status of the nematodes could cause significant oxidative damages and affect molecular, cellular and physiological processes of the organism.

### *4.2. Ionizing radiation-induced oxidative stress effects lead to differential regulation of genes required for cuticle morphology, protein degradation, lipid metabolism and gene expression*

In the current study, the overall redox balance of nematodes exposed to chronic gamma radiation was shown to be shifted towards a more oxidized status, since increased levels of ROS and a temporary but significant imbalance in the ratio of reduced glutathione to glutathione disulphide were measured. Within the "redox hypothesis" paradigm [43], much of the toxicity of oxidative stress could result from an oxidative shift in redox state within one or more cellular compartments. This shift might transiently disrupt redox signalling as well as perturb the regular function of redox regulated proteins within these compartments. The result could still be pathological oxidative damage to cellular components, even though the cause could be indirect. Therefore, we anticipated a significant change in the transcriptome profile of irradiated nematodes, as a response to the observed increased levels of ROS and AODs.

As hypothesised, the transcriptome analysis performed on nematodes exposed to 100 mGy $h^{-1}$ revealed differential modulation of genes involved in oxidation-reduction processes and accordingly a significant enhancement of functions related to stress response (Sections 3.2.1-3.2.2).

In line with the results from the *sod1::gfp* reporter strain and the two ratiometric biosensors adopted in our study, RNA sequencing revealed dysregulation of genes involved in AOD system such as *sod-1*, *ctl-1*, *glrx-10*, *gst-20*, *trx-2* and *trxr-2*. Moreover, changes in the redox balance affected glutathione metabolism, by up-regulation of glutathione *de novo* synthesis (Section 3.2.2).

Oxidative stress response was the most up-regulated phenotypical variant gene category observed, followed by lipid metabolism, cuticle morphology and protein degradation (Fig. 8, Table S7), all functions that have been previously correlated to oxidative damage in *C. elegans* [66], which corroborates that chronic gamma radiation does cause an oxidative stress type transcriptional response.

Chronic exposure to 100 mGy $h^{-1}$ of ionizing gamma radiation (total dose ~7.2 Gy) induced up-regulation of 53 genes related to structural constituent of cuticle, collagen trimmer and moulting cycle. As suggested by Shin and co-authors (2011), this significant enrichment may indicate the involvement of collagens in the adaptive mechanism response against the ionizing radiation-induced oxidative stress. In this organism, the cuticle represents the barrier between the animal and the external environment, therefore it may have a direct protective function towards environmental perturbations as well as being indirectly regulated in response to ROS production and oxidative damage. Moreover, accumulation or excess of collagen has been shown to cause radiation-induced fibrosis, as well as to be a response to loss of redox-sensitive control during the inflammatory or proliferative stage [64].

Proteins segregation and degradation has also been addressed as a major target of ionizing radiation-induced oxidative damage, particularly, the carbonylation damage is unrepairable and when this impairs the activity of key proteins, such as those needed to repair and replicate the DNA, cell survival is endangered [19,58]. Consistently, the differential regulation of 12 genes involved in protein ubiquitination activity

(*C17H11.6*, *mib-1*, *plr-1*, *rle-1*, *siah-1*, *skr-16*, *smo-1*, *ubc-15*, *ubc-20*, *ubc-3*, *ubl-1*, *urm-1*), together with 6 genes encoding for proteasome subunits and protease activity (*asp-1*, *pbs-1*, *pbs-2*, *pbs-5*, *psmd-9*, *try-10*) gave indication of protein damage effects under exposure to chronic gamma radiation. This result was further validated by 17 DEGs identified in the over-represented category "Protein degradation variant" resulting from the oxidative-stress induced phenotype analysis (Table S7).

Excessive ROS formation can also affect lipids, in particular the oxidative deterioration of polyunsaturated fatty acids present in cellular membranes can lead to membrane destabilization and therefore further oxidative damage to biomolecules [32]. Consistent with the increased levels of $H_2O_2$ measured with the *HyPer* biosensor, we observed effects on lipids through the identification of more than 50 DEGs involved in lipid metabolism (Table S7), the up-regulation of 86 genes involved in membrane-enclosed lumen, 45 and 42 genes involved in endosome and lysosome-related morphology, respectively (Tables 1 and 2, Table S5). These results suggest that under chronic exposure to ionizing gamma radiation, the modulation of processes involved in maintenance, biosynthesis and accumulation of lipids is a further response to ROS production, as well as associated to effects on cell and organelle's membrane.

To further validate the hypothesis that the increased ROS levels was among the molecular initiating events responsible for the observed redox imbalance and the modulation of the nematode's transcription profile, we found 85 genes in common with wild-type oxidative stressed after exposure to Paraquat from Shin and co-authors (2011) ("N2 oxidative stressed" category, Fig. 8 and Table S7). These genes were mostly involved in collagen production, mitochondrial functions, ATP synthesis, chromatin modification (histones and methyltransferase activity), ribosomal functions, response to heat stress and ubiquitination; giving further evidence of the specific mode of action of ionizing gamma radiation in terms of oxidative damage on a molecular and cellular level.

Furthermore, as a consequence of changes in the physiological process of cellular signalling, we observed a significant enrichment in molecular functions required for the modulation of the gene expression (Section 3.2.1), including chromatin remodelling and transcriptional regulation. Molecular functions related to chromatin domains, transcription, post-transcriptional modifications, RNA transport and processing were significantly over-represented (Table 1, Fig. 9), giving indication of changes in the gene expression profile of nematodes under exposure to chronic gamma radiation.

These findings demonstrate that a tolerant organism, like the nematode *C. elegans*, is able to effectively respond to a persistent stress condition, such as a chronic irradiation during the entire larval development, by modulating its biological, cellular and molecular functions (Fig. 9), in order to maintain the organism homeostasis, however this comes to the cost of energy expenditure and reproductive fitness (Fig. 1).

### 4.3. Transcriptomic analysis reveals mitochondrial functions and ATP synthesis as targets of ionizing gamma radiation in C. elegans

Exposure to ionizing radiation is associated with the manifestation of mitochondrial dysfunction [4]. Oxidative phosphorylation is susceptible to this stressor, due to the alteration of the complexes involved in the Electron Transport Chain (ETC) and the ATP synthase activity [44]. As a response to oxidative stress, the mtDNA copy number increases [39] and in order to ensure stable levels of ATP also the mitochondrial mass increases [20]. Dysfunctions in the ETC leads to further production of mitochondrial ROS, and conversely, cells deficient in mitochondrial ETC (rho$^{(o)}$ cells) do not show radiation-induced ROS production [47]. Consistently, we observe compelling down-regulation of all ten protein encoding genes out of the 12 genes required for the assembly of the Mitochondrial respiratory chain (*COX1*, *COX2*, *COX3*, *ND1*, *ND2*, *ND3*, *ND4*, *ND5*, *CYTB* and *ATP6*) (Fig. 8, Table S7). Furthermore, we identified down-regulation of 10 genes encoding for small and large mitochondrial ribosomal proteins (mrpl-10, mrpl-18, mrpl-28, mrpl-36, mrpl-41, mrpl-49, mrpl-50, mrps-17, mrps-21, mrps-23), which are required for the proper assembly and function of ETC mediated energy production [6]. We also observed differential regulation of genes involved in Mitochondrial metabolism (*immt-1*, *let-2*, *ril-1*, *cox-4*, *sdha-1*, *madd-2*, *unc-52*, *rict-1*, *pgs-1*, *bcs-1*, *mics-1*, *mspn-1*, *mttu-1*, *nuaf-1*, *rad-8*, *ZK1128.1*), genome maintenance (*C27H6.9*), protein import (*tomm-22*, *tomm-7*, *ddp-1*), Energy expenditure (*sdha-1*, *cox-5B*, *rict-1*, *sdhd-1*, *T02H6.11*) (Table S7) and ATP synthesis (*asb-2*, *asg-2*,

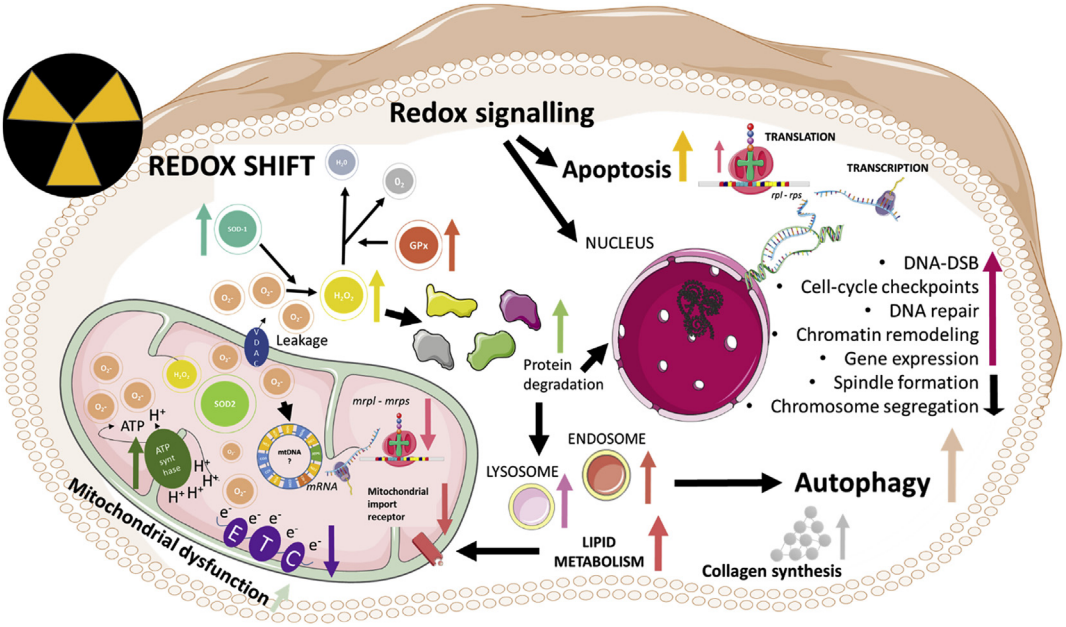


**Fig. 9.** Conceptual model of cellular and molecular processes induced (↑) or inhibited (↓) after 72 h of chronic exposure to gamma radiation (100 mGy h$^{-1}$, total dose ~7.2 Gy) in the nematode *C. elegans*.
ETC: Electron Transport Chain. VDAC: Voltage-Dependent Anion Channel. SOD: Superoxide Dismutase. *mrpl – mrps*: Mitochondrial Ribosomal Protein Large – Small subunit. mtDNA: mitochondrial DNA. GPx: Glutathione Peroxidases. *rpl – rps*: Ribosomal Protein Large – Small subunit. DNA-DSB: DNA Double Strand Break.

*atp-1*, *atp-4*, *atp-5*, *catp-1*, vha-3 and *F58F12.1*) (Fig. 9). Differential regulation of the mitochondrial cytochrome *b* and its subunits (*CYTB*, *hpo-19*, *sdhd-1*, *ucr-2.1*) was also observed, specifically the inhibition of cytochrome *b*5 reductase (*hpo-19*) has previously shown to induce decreased levels of poly-unsaturated fatty acids (PUFAs), which leads to decreased fat accumulation, reduced brood size and impaired development [83].

Mitochondrial dysfunctions in irradiated cells can significantly contribute to perturbation in the physiological redox reactions and signalling [44]. Such perturbation can lead to signalling cascades which can induce a multitude of other non-targeted responses such as apoptosis, autophagy, nuclear DNA damage, genomic instability and other degenerative conditions [16,52,64,67]. Thus, consistent with the induced AODs and ROS production, measured in the current study, the changes observed in the nematode transcriptome profile, with respect to mitochondrial functions and ATP production, were a clear evidence of the mitochondrial vulnerability under exposure to ionizing radiation and a signal for late consequences on other cellular, molecular and biological functions.

### *4.4. Ionizing radiation-induced DNA damage leads to histones up-regulation and methylation, defective chromosome segregation, programmed cell death, and impairment of nervous system and embryonic development*

Upon severe stress condition, survival is dependent on the ability of the cell to adapt or resist the stress, by for instance repairing or replacing the damaged molecules [26]. Beyond the well-known DNA repair mechanisms of homologous recombination (HR) and non-homologous end-joining (NHEJ), emerging evidence indicates that also epigenetic changes can enable adaptation responses in the surviving cells [71,79]. Consistent with this hypothesis, we identified a significant up-regulation of 20 core histone encoding genes (H3, H4), which might represent a response to DNA damage and, in this sense, a protective mechanism via the promotion of chromatin condensation [73]. Furthermore, methylation of lysine residues on histones can play an important role in determining the repair pathway upon double-strand breaks (DSBs) [79]. In good accordance, we identified a significant up-regulation of *dot-1.1*, *set-9*, *set-16* and *set-26*, which encode for histone-lysine N-methyltransferases. The genes *set-9* and *set-26* are also required for longevity, germline development and heat stress response, giving further evidence of the connection between oxidative damage and adverse effects exerted by chronic irradiation on the reproductive system.

Consistent with our previous study [55], we found further indication of adverse effects exerted by chronic gamma irradiation on chromosome segregation, mitotic and meiotic cell-cycle, spindle formation and embryonic development (Fig. S7; Tables 1 and 2, Table S6). In both studies, these effects were accompanied by impairment of the nematodes reproductive capacity (Fig. 1b), which was further supported, in the current study, by the down-regulation of more than 300 genes related to the reproductive system (Fig. S. 7.c). Specifically, we found a differential regulation of cellular and molecular functions related to reproduction, such as gamete development and fertilization, cytokinesis, sister chromatid segregation defective in early embryo, diplotene absent during oogenesis, gonad small, reproductive system development, meiotic chromosome segregation, spindle position and orientation and aneuploidy. As already shown in our previous study, where enhanced germ cell apoptosis and impaired spermatogenesis lead to reprotoxicity [55], all these over-represented categories gave further evidence of the persistent adverse effects induced by chronic gamma irradiation on the meiotic process, which subsequently leads to loss of the reproductive fitness.

Oxidative metabolic processes that produce ROS are important for the regulation of the cell-cycle functions, proliferation and differentiation [64]. Hence, metabolic defects that disrupt signalling function of ROS could be detrimental to a multitude of cellular processes. In line with our previous research [55], in the current study, chronic gamma irradiation showed effects on the cell-cycle via induction of genomic instability and DNA damage through the differential expression of genes involved in DNA double strand break (*dsb-3*), cell-cycle checkpoint (*hus-1*, *cdc-25.2*, *cdc-37*, *cdc-48.3*, *chk-1*, *cki-1*) and DNA repair (*rad-54*, *chd-7*, *laf-1*, *pif-1*, *snrp-200*, *ssl-1*, *pms-2*, *nth-1*, *polk-1*, *rpa-2* and *unc-51*). A cell damaged beyond repair will be destined to apoptosis; increased levels of ROS formed inside the mitochondrion have the potential to induce downstream regulation of genes required for apoptosis by the early ROS-dependent signalling pathway [67]. Consistently, we found 87 differentially expressed genes involved in programmed cell death (Fig. 8, Table S7), among them *egl-1* and *hus-1*, which are clear markers of DNA damage-induced apoptosis [37].

On the other hand, proliferative disorders due to differential regulation of the cell-cycle under redox cycle control, are addressed as the cause of many dysfunctions as well as diseases, including cancer and neurodegenerative disorders [64]. Consistently, a significant modulation of genes related to nervous system functions was identified in our gene expression analysis, through the up-regulation of genes involved in neurogenesis, neuronal development, neuron projection guidance and neuronal outgrowth (Tables 1 and 2, Table S6). These results suggest an effect exerted by ionizing radiation on somatic cells. Specifically, and in contrast to the germline, adverse effects on somatic cells might induce a savage beyond repair as indicated by the categories apoptosis fails to occur, defective locomotion (sluggish), endosome and lysosome-related morphology variants (Table 2) and autophagy related genes (*unc-51*, *atg-3*, *atg-9*, *ces-2* and *rab-7*). In particular, the lysosome-mediated self-degradation process of autophagy can be used to supply the cells with energy or provide building block for the synthesis of macromolecules, under stress condition [25]. This mechanism is known to be specific for terminally differentiated cells, where it is required for the effective elimination of damaged, non-functional macromolecules and organelles, in order to avoid this cellular toxins to interfere with cellular functions [78]. Moreover, the over-activation of autophagy in cells of the nervous system has been suggested as the cause of “physiological” death [72]. Autophagy and apoptosis are two intertwined processes required redundantly for viability and normal development in *C. elegans* [25]. In line with the significantly enhanced embryonic DNA damage and reduced somatic growth, observed in parentally irradiated nematodes from our previous study [55], the differential regulation of genes related to autophagy, programmed cell death, embryonic and post-embryonic development (Fig. S7, Fig. 8, Table 1), strongly suggests that the effects of chronic gamma irradiation persist on the progeny of irradiated nematodes.

Taken together these results demonstrate the ability of *C. elegans* to activate its wide range of AODs and protective mechanisms against increased levels of ROS following chronic gamma irradiation throughout its life cycle. This did however present a stress condition able to induce changes in the physiological oxidants levels, which lead to a comprehensive modulation of cellular and molecular functions (Fig. 9), leading up to adverse effects on energy production/expenditure and reproductive capacity as well as persistent damage on the parentally irradiated offspring [55].

## 5. Conclusion

In the radioresistant nematode *C. elegans*, chronic exposure to ionizing gamma radiation, during larval development, significantly enhances the levels of ROS and induces activation of AODs. At doses $\leq 10$ mGy $h^{-1}$ (total doses $\leq 0.8$ Gy) nematodes demonstrate to tolerate chronic gamma irradiation, while at doses $\geq 40$ mGy $h^{-1}$ (total doses $\geq 2.9$ Gy) , the observed redox shift in the cell induces oxidative damage and changes in the redox signalling functions, modulating a cascade of molecular and cellular processes in the entire organism with adverse consequences for its reproductive system. Specifically, oxidative damage of proteins, lipids and DNA is suggested as the cause of

mitochondrial dysfunctions, impaired energy production, autophagy induction, enhanced programmed cell death and defective meiosis, which leads to impairment of the reproductive fitness and potential adverse effects on the progeny. Findings from the current study provide detailed information of the consequences of chronic exposure to ionizing radiation, as well as the important role of redox balance and signalling for the cellular homeostasis, particularly in the gonads. Future research should be focused on the effects of this imbalance at the mitochondrial level, with emphasis on the potential adverse effects of ROS on the ATP production and the mitochondrial genome.

## Funding

This work was supported by the Norwegian University of Life Sciences (NMBU) through a PhD scholarship and by the Research Council of Norway through its Centre of Excellence (CoE) “Centre for Environmental Radioactivity” (CERAD, project No. 223268).

## Acknowledgments

We are grateful to Dr. Marina Ezcurra and Prof. David Gems from the Institute of Healthy Ageing Genetics (University College London) for providing the *C. elegans* reporter strain *sod-1::gfp* (GA508 wuls54[pPD95.77 sod-1::GFP, rol-6(su1006)]) and Dr. Braeckman from the Laboratory for Ageing Physiology and Molecular Evolution (University of Ghent, Belgium) for providing the *C. elegans* biosensors *Grx1-roGFP2* and *HyPer*. We also thank Fabian Grammes for bioinformatics assistance and Simen Gylterud Owe, YeonKyeong Lee, Hilde Raanaas Kolstad and Lene Cecilie Hermansen for kind assistance and help during the microscopy analysis.

## Appendix A. Supplementary data

Supplementary data to this article can be found online at https://doi.org/10.1016/j.freeradbiomed.2019.11.037.

## References

[1] C. Adam-Guillermin, S. Pereira, C. Della-Vedova, T. Hinton, J. Garnier-Laplace, Genotoxic and reprotoxic effects of tritium and external gamma irradiation on aquatic animals, in: D.M. Whitacre (Ed.), Reviews of Environmental Contamination and Toxicology, Springer, New York, NY, 2012(New York).
[2] D. Angeles-Albores, R.Y. Lee, J. Chan, P.W. Sternberg, Tissue enrichment analysis for *C. elegans* genomics, BMC Bioinf. 17 (2016) 366.
[3] D. Angeles-Albores, R.Y. Lee, J. Chan, P.W. Sternberg, Phenotype and Gene Ontology Enrichment as Guides for Disease Modeling in C. elegans, (2017), p. 106369 BioRxiv.
[4] E.I. Azzam, J.-P. Jay-Gerin, D. Pain, Ionizing radiation-induced metabolic oxidative stress and prolonged cell injury, Cancer Lett. 327 (2012) 48–60.
[5] P. Back, W.H. DE Vos, G.G. Depuydt, F. Matthijssens, J.R. Vanfleteren, B.P. Braeckman, Exploring real-time in vivo redox biology of developing and aging Caenorhabditis elegans, Free Radic. Biol. Med. 52 (2012) 850–859.
[6] J.M. Berg, J.L. Tymoczko, L. Stryer, Biochemistry, 5th, WH Freeman, New York, 2006.
[7] L. Bergendi, L. Beneš, Z. Ďuračková, M. Ferenčik, Chemistry, physiology and pathology of free radicals, Life Sci. 65 (1999) 1865–1874.
[8] H. Bjerke, P.O. Hetland, Dosimetri ved FIGARO gammaanlegget ved Nmbu, ÅS. *Målerapport fra oppmåling av doseraten i strålefeltet fra kobolt-60*, 2 (2014) NRPA Technical Document Series.
[9] N.R. Brady, A. Hamacher-Brady, H.V. Westerhoff, R.A. Gottlieb, A wave of reactive oxygen species (ROS)-induced ROS release in a sea of excitable mitochondria, Antioxidants Redox Signal. 8 (2006) 1651–1665.
[10] B. Braeckman, P.U. Back, F.G.E. Matthijssens, A.E. Olsen, M.S.E. Gill, Oxidative stress, in: S.I.S. Rattan (Ed.), Healthy Ageing and Longevity, Springer, 2017.
[11] B.P. Braeckman, A. Smolders, P. Back, S. DE Henau, In vivo detection of reactive oxygen species and redox status in Caenorhabditis elegans, Antioxidants Redox Signal. 25 (2016) 577–592.
[12] M.D. Brand, The sites and topology of mitochondrial superoxide production, Exp. Gerontol. 45 (2010) 466–472.
[13] A. Buisset-Goussen, B. Goussen, C. Della-Vedova, S. Galas, C. Adam-Guillermin, C. Lecomte-Pradines, Effects of chronic gamma irradiation: a multigenerational study using *Caenorhabditis elegans*, J. Environ. Radioact. 137 (2014) 190–197.
[14] F. Cabreiro, D. Ackerman, R. Doonan, C. Araiz, P. Back, D. Papp, B.P. Braeckman, D. Gems, Increased life span from overexpression of superoxide dismutase in Caenorhabditis elegans is not caused by decreased oxidative damage, Free Radic. Biol. Med. 51 (2011) 1575–1582.
[15] Q. Chen, Y.C. Chai, S. Mazumder, C. Jiang, R.M. Macklis, G.M. Chisolm, A. Almasan, The late increase in intracellular free radical oxygen species during apoptosis is associated with cytochrome c release, caspase activation, and mitochondrial dysfunction, Cell Death Differ. 10 (2003) 323–334.
[16] K.-M. Choi, C.-M. Kang, E.S. Cho, S.M. Kang, S.B. Lee, H.-D. Um, Ionizing radiation-induced micronucleus formation is mediated by reactive oxygen species that are produced in a manner dependent on mitochondria, Nox1, and JNK, Oncol. Rep. 17 (2007) 1183–1188.
[17] A. Chomyn, G. Attardi, Mitochondrial gene products, Curr. Top. Bioenerg.: Struct. Biogenesis. Assemb. Energy Transducing Enzyme Syst. 15 (2014) 295.
[18] A. Daiber, Redox signaling (cross-talk) from and to mitochondria involves mitochondrial pores and reactive oxygen species, Biochim. Biophys. Acta 1797 (2010) 897–906.
[19] M.J. Daly, Death by protein damage in irradiated cells, DNA Repair 11 (2012) 12–21.
[20] D. Dayal, S.M. Martin, K.M. Owens, N. Aykin-Burns, Y. Zhu, A. Boominathan, D. Pain, C.L. Limoli, P.C. Goswami, F.E. Domann, D.R. Spitz, Mitochondrial complex II dysfunction can contribute significantly to genomic instability after exposure to ionizing radiation, Radiat. Res. 172 (2009) 737–745 9.
[21] A. Dobin, C.A. Davis, F. Schlesinger, J. Drenkow, C. Zaleski, S. Jha, P. Batut, M. Chaisson, T.R. Gingeras, STAR: ultrafast universal Rna-seq aligner, Bioinformatics 29 (2013) 15–21.
[22] R. Doonan, J.J. Mcelwee, F. Matthijssens, G.A. Walker, K. Houthoofd, P. Back, A. Matscheski, J.R. Vanfleteren, D. Gems, Against the oxidative damage theory of aging: superoxide dismutases protect against oxidative stress but have little or no effect on life span in Caenorhabditis elegans, Genes Dev. 22 (2008) 3236–3241.
[23] S. Dröse, U. Brandt, Molecular Mechanisms of Superoxide Production by the Mitochondrial Respiratory Chain. Mitochondrial Oxidative Phosphorylation, Springer, 2012.
[24] C. Dubois, C. Lecomte, S.P.D. Ruys, M. Kuzmic, C. Della-Vedova, N. Dubourg, S. Galas, S. Frelon, Precoce and opposite response of proteasome activity after acute or chronic exposure of C. elegans to γ-radiation, Sci. Rep. 8 (2018) 11349.
[25] P. Erdélyi, É. Borsos, K. Takács-Vellai, T. Kovács, A.L. Kovács, T. Sigmond, B. Hargitai, L. Pásztor, T. Sengupta, M. Dengg, I. Pécsi, J. Tóth, H. Nilsen, B.G. Vértessy, T. Vellai, Shared developmental roles and transcriptional control of autophagy and apoptosis in *Caenorhabditis elegans*, J. Cell Sci. 124 (2011) 1510–1518.
[26] T. Finkel, N.J. Holbrook, Oxidants, oxidative stress and the biology of ageing, Nature 408 (2000) 239.
[27] D. Gems, R. Doonan, Oxidative Stress and Aging in the NematodeCaenorhabditis Elegans. *Oxidative* Stress in Aging, Springer, 2008.
[28] A. Gomes, E. Fernandes, J.L. Lima, Fluorescence probes used for detection of reactive oxygen species, J. Biochem. Biophys. Methods 65 (2005) 45–80.
[29] T. Gomes, Y. Song, D.A. Brede, L. Xie, K.B. Gutzkow, B. Salbu, K.E. Tollefsen, Gamma radiation induces dose-dependent oxidative stress and transcriptional alterations in the freshwater crustacean Daphnia magna, Sci. Total Environ. 628 (2018) 206–216.
[30] T. Gomes, L. Xie, D. Brede, O.-C. Lind, K.A. Solhaug, B. Salbu, K.E. Tollefsen, Sensitivity of the green algae Chlamydomonas reinhardtii to gamma radiation: photosynthetic performance and ROS formation, Aquat. Toxicol. 183 (2017) 1–10.
[31] X. Guo, J. Sun, P. Bian, L. Chen, F. Zhan, J. Wang, A. Xu, Y. Wang, T.K. Hei, L. Wu, Radiation-induced bystander signaling from somatic cells to germ cells in Caenorhabditis elegans, Radiat. Res. 180 (2013) 268–275.
[32] B. Halliwell, J.M. Gutteridge, Free Radicals in Biology and Medicine, Oxford University Press, USA, 2015.
[33] D. Han, F. Antunes, R. Canali, D. Rettori, E. Cadenas, Voltage-dependent anion channels control the release of the superoxide anion from mitochondria to cytosol, J. Biol. Chem. 278 (2003) 5557–5563.
[34] P.S. Hartman, V.J. Simpson, T. Johnson, D. Mitchell, Radiation sensitivity and DNA repair in Caenorhabditis elegans strains with different mean life spans, Mutat. Res. Lett. 208 (1988) 77–82.
[35] T. Hertel-Aas, G. Brunborg, A. Jaworska, B. Salbu, D.H. Oughton, Effects of different gamma exposure regimes on reproduction in the earthworm Eisenia fetida (Oligochaeta), Sci. Total Environ. 412–413 (2011) 138–147.
[36] T. Hertel-Aas, D.H. Oughton, A. Jaworska, H. Bjerke, B. Salbu, G. Brunborg, Effects of chronic gamma irradiation on reproduction in the earthworm Eisenia fetida (Oligochaeta), Radiat. Res. 168 (2007) 515–526.
[37] E.R. Hofmann, S. Milstein, S.J. Boulton, M. Ye, J.J. Hofmann, L. Stergiou, A. Gartner, M. Vidal, M.O. Hengartner, *Caenorhabditis elegans* Hus-1 is a DNA damage checkpoint protein required for genome stability and egl-1-mediated apoptosis, Curr. Biol. 12 (2002) 1908–1918.
[38] S. Honnen, Caenorhabditis elegans as a powerful alternative model organism to promote research in genetic toxicology and biomedicine, Arch. Toxicol. 91 (2017) 2029–2044.
[39] A. Hori, M. Yoshida, T. Shibata, F. Ling, Reactive oxygen species regulate DNA copy number in isolated yeast mitochondria by triggering recombination-mediated replication, Nucleic Acids Res. 37 (2008) 749–761.
[40] S. Hurem, T. Gomes, D.A. Brede, E. LINDBO Hansen, S. Mutoloki, C. Fernandez, C. Mothersill, B. Salbu, Y.A. Kassaye, A.-K. Olsen, D. Oughton, P. Alestrom, J.L. Lyche, Parental gamma irradiation induces reprotoxic effects accompanied by genomic instability in zebrafish (Danio rerio) embryos, Environ. Res. 159 (2017) 564–578.
[41] International, O., For, Standardization, Water quality—determination of the toxic effect of sediment and soil samples on growth, fertility and reproduction of

*Caenorhabditis elegans(Nematoda)*, (2010) International Organization for Standardization (ISO) 10872:2010.
[42] A.D. Johnston, P.R. Ebert, The redox system in C. elegans, a phylogenetic approach, J. Toxicol. 2012 (2012) 20.
[43] D.P. Jones, Radical-free biology of oxidative stress, Am. J. Physiol. Cell Physiol. 295 (2008) C849–C868.
[44] W.W.-Y. Kam, R.B. Banati, Effects of ionizing radiation on mitochondria, Free Radic. Biol. Med. 65 (2013) 607–619.
[45] N. Khanna, C. CRESSMAN Iii, C. Tatara, P. Williams, Tolerance of the nematode Caenorhabditis elegans to ph, salinity, and hardness in aquatic media, Arch. Environ. Contam. Toxicol. 32 (1997) 110–114.
[46] A. Krisko, M. Leroy, M. Radman, M. Meselson, Extreme anti-oxidant protection against ionizing radiation in bdelloid rotifers, Proc. Natl. Acad. Sci. U. S. A. 109 (2012) 2354–2357.
[47] J.K. Leach, G. VAN Tuyle, P.-S. Lin, R. Schmidt-Ullrich, R.B. Mikkelsen, Ionizing radiation-induced, mitochondria-dependent generation of reactive oxygen/nitrogen, Cancer Res. 61 (2001) 3894–3901.
[48] R.Y.N. Lee, K.L. Howe, T.W. Harris, V. Arnaboldi, S. Cain, J. Chan, W.J. Chen, P. Davis, S. Gao, C. Grove, WormBase 2017: molting into a new stage, Nucleic Acids Res. 46 (2017) D869–D874.
[49] J.A. Lewis, J.T. Fleming, Chapter 1 basic culture methods, in: H.F. Epstein, D.C. Shakes (Eds.), Methods in Cell Biology, Academic Press, 1995.
[50] O.C. Lind, D.H. Oughton, B. Salbu, The NMBU FIGARO low dose irradiation facility, Int. J. Radiat. Biol. 95 (2019) 76–81.
[51] E. Lindbo Hansen, P.O.H. Ø, Air Kerma Measurements with Landauer nanoDots in Cs-137 and Co-60 Beams, Teknisk Dokument Nr, vol 8, Norwegian Radiation Protection Authority, 2017.
[52] S.L. Lomonaco, S. Finniss, C. Xiang, A. Decarvalho, F. Umansky, S.N. Kalkanis, T. Mikkelsen, C. Brodie, The induction of autophagy by γ-radiation contributes to the radioresistance of glioma stem cells, Int. J. Cancer 125 (2009) 717–722.
[53] M.I. Love, S. Anders, V. Kim, W. Huber, Rna-Seq workflow: gene-level exploratory analysis and differential expression, FResearch 4 (2015).
[54] S.C. Lu, Regulation of glutathione synthesis, Mol. Asp. Med. 30 (2009) 42–59.
[55] E. Maremonti, D.M. Eide, D.H. Oughton, B. Salbu, F. Grammes, Y.A. Kassaye, R. Guédon, C. Lecomte-Pradine, D.A. Brede, Gamma radiation induces life stage-dependent reprotoxicity in Caenorhabditis elegans via impairment of spermatogenesis, Sci. Total Environ. (2019) 133835.
[56] A.J. Meyer, T.P. Dick, Fluorescent protein-based redox probes, Antioxidants Redox Signal. 13 (2010) 621–650.
[57] D.C. Montgomery, E.A. Peck, G.G. Vining, Introduction to Linear Regression Analysis, John Wiley & Sons, 2012.
[58] T. Nyström, Role of oxidative carbonylation in protein quality control and senescence, EMBO J. 24 (2005) 1311–1317.
[59] F. Parisot, J.-P. Bourdineaud, D. Plaire, C. Adam-Guillermin, F. Alonzo, DNA alterations and effects on growth and reproduction in Daphnia magna during chronic exposure to gamma radiation over three successive generations, Aquat. Toxicol. 163 (2015) 27–36.
[60] A. Pompella, A. Visvikis, A. Paolicchi, V.D. Tata, A.F. Casini, The changing faces of glutathione, a cellular protagonist, Biochem. Pharmacol. 66 (2003) 1499–1503.
[61] M. Porta-De-La-Riva, L. Fontrodona, A. Villanueva, J. Ceron, Basic Caenorhabditis elegans methods: synchronization and observation, J. Vis. Exp. (2012) e4019.
[62] J.A. Reisz, N. Bansal, J. Qian, W. Zhao, C.M. Furdui, Effects of ionizing radiation on biological molecules—mechanisms of damage and emerging methods of detection, Antioxidants Redox Signal. 21 (2014) 260–292.
[63] P.A. Riley, Free radicals in biology: oxidative stress and the effects of ionizing radiation, Int. J. Radiat. Biol. 65 (1994) 27–33.
[64] E.H. Sarsour, M.G. Kumar, L. Chaudhuri, A.L. Kalen, P.C. Goswami, Redox control of the cell cycle in health and disease, Antioxidants Redox Signal. 11 (2009) 2985–3011.
[65] F.Q. Schafer, G.R. Buettner, Redox environment of the cell as viewed through the redox state of the glutathione disulfide/glutathione couple, Free Radic. Biol. Med. 30 (2001) 1191–1212.
[66] H. Shin, H. Lee, A.P. Fejes, D.L. Baillie, H.-S. Koo, S.J. Jones, Gene expression profiling of oxidative stress response of C. elegans aging defective AMPK mutants using massively parallel transcriptome sequencing, BMC Res. Notes 4 (2011) 34.
[67] C. Sidoti-DE Fraisse, V. Rincheval, Y. Risler, B. Mignotte, J.-L. Vayssière, Tnf-α activates at least two apoptotic signaling cascades, Oncogene 17 (1998) 1639.
[68] J.T. Smith, N.J. Willey, J.T. Hancock, Low dose ionizing radiation produces too few reactive oxygen species to directly affect antioxidant concentrations in cells, Biol. Lett. 8 (2012) 594–597.
[69] D.R. Spitz, E.I. Azzam, J.J. Li, D. Gius, Metabolic oxidation/reduction reactions and cellular responses to ionizing radiation: a unifying concept in stress response biology, Cancer Metastasis Rev. 23 (2004) 311–322.
[70] K.B. Storey, Oxidative stress: animal adaptations in nature, Braz. J. Med. Biol. Res. 29 (1996) 1715–1733.
[71] I. Szumiel, Ionizing radiation-induced oxidative stress, epigenetic changes and genomic instability: the pivotal role of mitochondria, Int. J. Radiat. Biol. 91 (2015) 1–12.
[72] K. TAKÁCS-Vellai, A. Bayci, T. Vellai, Autophagy in neuronal cell loss: a road to death, Bioessays 28 (2006) 1126–1131.
[73] H. Takata, T. Hanafusa, T. Mori, M. Shimura, Y. Iida, K. Ishikawa, K. Yoshikawa, Y. Yoshikawa, K. Maeshima, Chromatin compaction protects genomic DNA from radiation damage, PLoS One 8 (2013) e75622.
[74] Y. Tateishi, E. Sasabe, E. Ueta, T. Yamamoto, Ionizing irradiation induces apoptotic damage of salivary gland acinar cells via NADPH oxidase 1-dependent superoxide generation, Biochem. Biophys. Res. Commun. 366 (2008) 301–307.
[75] J.F. Turrens, Mitochondrial formation of reactive oxygen species, J. Physiol. 552 (2003) 335–344.
[76] United States Environmental Protection Agency, Methods for Measuring the Acute Toxicity of Effluents and Receiving Waters to Freshwater and Marine Organisms, U. E, fifth ed., (2002) Epa-821-R-02-012.
[77] UNSCEAR, Sources and Effects of Ionizing Radiation: Report to the General Assembly, with Scientific Annexes, United Nations Publications, 1996.
[78] T. Vellai, K. Takács-Vellai, M. Sass, D. Klionsky, The regulation of aging: does autophagy underlie longevity? Trends Cell Biol. 19 (2009) 487–494.
[79] S. Wei, C. Li, Z. Yin, J. Wen, H. Meng, L. Xue, J. Wang, Histone methylation in DNA repair and clinical practice: new findings during the past 5-years, J. Cancer 9 (2018) 2072–2081.
[80] G. Wu, Y.-Z. Fang, S. Yang, J.R. Lupton, N.D. Turner, Glutathione metabolism and its implications for health, J. Nutr. 134 (2004) 489–492.
[81] L. Xie, K.A. Solhaug, Y. Song, D.A. Brede, O.C. Lind, B. Salbu, K.E. Tollefsen, Modes of action and adverse effects of gamma radiation in an aquatic macrophyte Lemna minor, Sci. Total Environ. 680 (2019) 23–34.
[82] T. Yamamori, H. Yasui, M. Yamazumi, Y. Wada, Y. Nakamura, H. Nakamura, O. Inanami, Ionizing radiation induces mitochondrial reactive oxygen species production accompanied by upregulation of mitochondrial electron transport chain function and mitochondrial content under control of the cell cycle checkpoint, Free Radic. Biol. Med. 53 (2012) 260–270.
[83] Y. Zhang, H. Wang, J. Zhang, Y. Hu, L. Zhang, X. Wu, X. Su, T. Li, X. Zou, B. Liang, The cytochrome b5 reductase Hpo-19 is required for biosynthesis of polyunsaturated fatty acids in Caenorhabditis elegans, Biochim. Biophys. Acta Mol. Cell Biol. Lipids 1861 (2016) 310–319.